



HAL
open science

Regional-scale analysis of carbon and water cycles on managed grassland systems

Shaoxiu Ma, Romain Lardy, Anne-Isabelle Graux, Haythem Ben Touhami, Katja Klumpp, Raphaël Martin, Gianni Bellocchi

► **To cite this version:**

Shaoxiu Ma, Romain Lardy, Anne-Isabelle Graux, Haythem Ben Touhami, Katja Klumpp, et al.. Regional-scale analysis of carbon and water cycles on managed grassland systems. *Environmental Modelling and Software*, Elsevier, 2015, 72, 10.1016/j.envsoft.2015.03.007 . hal-01210951

HAL Id: hal-01210951

<https://hal.archives-ouvertes.fr/hal-01210951>

Submitted on 28 May 2020

HAL is a multi-disciplinary open access archive for the deposit and dissemination of scientific research documents, whether they are published or not. The documents may come from teaching and research institutions in France or abroad, or from public or private research centers.

L'archive ouverte pluridisciplinaire **HAL**, est destinée au dépôt et à la diffusion de documents scientifiques de niveau recherche, publiés ou non, émanant des établissements d'enseignement et de recherche français ou étrangers, des laboratoires publics ou privés.

1
2
3
4
5 **1 Regional-scale analysis of carbon and water cycles on**
6
7 **2 managed grassland systems**
8

9 3

10 4

11 5

12
13 6 Shaoxiu Ma¹, Romain Lardy^{2,3}, Anne-Isabelle Graux⁴, Haythem Ben Touhami¹, Katja
14 Klumpp¹, Raphaël Martin¹, Gianni Bellocchi¹
15

16 8

17 9

18
19 10 ¹INRA, UR0874 Grassland Ecosystem Research, F-63039 Clermont-Ferrand, France
20

21 11 ²UMR 5505 IRIT, CNRS, University of Toulouse, France
22

23 12 ³UMR 1248 AGIR, INRA-INPT, Castanet-Tolosan, France
24

25 13 ⁴INRA – Agrocampus Ouest, UMR 1348 PEGASE, Domaine de la Prise, 35590
26 Saint-Gilles, France
27
28
29
30
31
32
33
34
35
36
37
38
39
40
41
42
43
44
45
46
47
48
49
50
51
52
53
54
55
56
57
58
59
60
61

1
2
3
4
5 **15 Abstract:**
6

7
8
9
10
11
12
13
14
15
16
17
18
19
20
21
22
23
24
25
26
27
28
29
30
31
32
33
34
35
36
37
38
39
40
41
42
43
44
45
46
47
48
49
50
51
52
53
54
55
56
57
58
59
60
61
62
63
64
65

16 Predicting regional and global carbon (C) and water dynamics on grasslands has
17 become of major interest, as grasslands are one of the most widespread vegetation
18 types worldwide, providing a number of ecosystem services (such as forage
19 production and C storage). The present study is a contribution to a regional-scale
20 analysis of the C and water cycles on managed grasslands. The mechanistic
21 biogeochemical model PaSim (Pasture Simulation model) was evaluated at 12
22 grassland sites in Europe. A new parameterization was obtained on a common set of
23 eco-physiological parameters, which represented an improvement of previous
24 parameterization schemes (essentially obtained via calibration at specific sites). We
25 found that C and water fluxes estimated with the parameter set are in good agreement
26 with observations. The model with the new parameters estimated that European
27 grassland are a sink of C with $213 \text{ g C m}^{-2} \text{ yr}^{-1}$, which is close to the observed net
28 ecosystem exchange (NEE) flux of the studied sites ($185 \text{ g C m}^{-2} \text{ yr}^{-1}$ on average).
29 The estimated yearly average gross primary productivity (GPP) and ecosystem
30 respiration (RECO) for all of the study sites are 1220 and $1006 \text{ g C m}^{-2} \text{ yr}^{-1}$,
31 respectively, in agreement with observed average GPP ($1230 \text{ g C m}^{-2} \text{ yr}^{-1}$) and RECO
32 ($1046 \text{ g C m}^{-2} \text{ yr}^{-1}$). For both variables aggregated on a weekly basis, the root mean
33 square error (RMSE) was $\sim 5\text{-}16 \text{ g C week}^{-1}$ across the study sites, while the goodness
34 of fit (R^2) was $\sim 0.4\text{-}0.9$. For evapotranspiration (ET), the average value of simulated
35 ET (415 mm yr^{-1}) for all sites and years is close to the average value of the observed
36 ET (451 mm yr^{-1}) by flux towers (on a weekly basis, $\text{RMSE} \sim 2\text{-}8 \text{ mm week}^{-1}$;

1
2
3
4
5 37 $R^2=0.3-0.9$). However, further model development is needed to better represent soil
6
7 38 water dynamics under dry conditions and soil temperature in winter. A quantification
8
9 39 of the uncertainties introduced by spatially generalized parameter values in C and
10
11 40 water exchange estimates is also necessary. In addition, some uncertainties in the
12
13 41 input management data call for the need to improve the quality of the observational
14
15 42 system.
16
17
18
19
20
21
22
23
24
25
26
27

28 **Key word:**

29
30
31 47 Carbon flux, eddy flux measurements, model evaluation, Pasture Simulation model
32
33 48 (PaSim), water balance
34
35 49
36
37
38
39
40
41
42
43
44
45
46
47
48
49
50
51
52
53
54
55
56
57
58
59
60
61
62
63
64
65

1
2
3
4
5
6
7
8
9
10
11
12
13
14
15
16
17
18
19
20
21
22
23
24
25
26
27
28
29
30
31
32
33
34
35
36
37
38
39
40
41
42
43
44
45
46
47
48
49
50
51
52
53
54
55
56
57
58
59
60
61
62
63
64
65

50 **Software availability**
51 Name of Software: Pasture Simulation model (PaSim)
52 Developer: INRA, UR0874 initiative; contact: Raphaël Martin
53 Contact Address: INRA, UR0874 Grassland Ecosystem Research, 63039
54 Clermont-Ferrand, France
55 Telephone: +33-4-73624872
56 E-mail: raphael.martin@clermont.inra.fr
57 Availability: On request to the authors
58 Cost: free for no-profit use
59 Program language: Fortran
60
61

1. Introduction

Accurate quantification of ecosystem carbon (C) and water fluxes over regions, continents, or the globe is essential for understanding the feedbacks between the terrestrial biosphere and the atmosphere in the context of global change and climate policy-making (Xiao et al., 2012; Ciais et al., 2013). In the last decades, significant progresses have been made in quantifying regional to global C and water fluxes by using ecosystem modelling (Jung et al., 2007; Xiao et al., 2009), atmospheric inverse modelling (Butler et al., 2010) and upscaling of flux observations from eddy covariance towers (Jung et al., 2011). In particular, integrated environmental modelling (Laniak et al., 2013) provides effective tools for studying C and water cycles in agricultural and natural systems. Ecosystem models have been intensively developed and used to estimate C and water exchanges between the atmosphere and biosphere (Bondeau et al., 1999; Churkina et al., 1999; Huntzinger et al., 2012; Warszawski et al., 2014). They represent the key processes (such as plant photosynthesis, ecosystem respiration and evapotranspiration) and climatic and management drivers (e.g. grazing, cutting and fertilization) that regulate energy and matter exchanges. However, most of the modelling efforts have focussed on forests (Bondeau et al., 1999; Schaefer et al., 2012; Wu et al., 2012) and croplands (Palosuo et al., 2011; Roetter et al., 2012; Wattenbach et al., 2010), while lesser attention was given to grasslands (Ciais et al., 2010).

Grasslands are a widespread vegetation type worldwide, covering nearly one-fifth of the world's land surface (24 million km²) (Suttie et al., 2005) and playing a significant

1
2
3
4
5 84 role in the global C cycle (Scurlock and Hall, 1998; Ciais et al., 2010). At global scale,
6
7
8 85 grasslands were estimated to be a net C sink of about 0.5 Pg C per year (Scurlock and
9
10 86 Hall, 1998), but with high spatial heterogeneity and considerable uncertainty on the
11
12 87 estimate of C exchange. Janssens et al. (2005) estimated that grasslands provide a C
13
14
15 88 sink of 66 ± 90 g C m⁻² yr⁻¹ over Europe. From an extensive network of flux towers,
16
17
18 89 Schulze et al. (2009) inferred a net C sink: net biome production (NBP) in European
19
20 90 grasslands of 57 ± 34 g C m⁻² yr⁻¹. However, grassland ecosystems are the most
21
22 91 uncertain components of the Europe-wide C balance in comparison to forests and
23
24
25 92 croplands because only few data and grassland-specific models are available (Ciais et
26
27
28 93 al., 2010). As a consequence, it is urgent to improve and evaluate grassland models
29
30
31 94 based on recently-available eddy flux data.

32
33
34 95 Over the last decades, grassland models were developed with different research foci.
35
36
37 96 CENTURY model was developed to simulate soil C, N, P, and S dynamics on a
38
39 97 monthly time step (Parton, 1988), with an updated version (DayCent) working on a
40
41
42 98 daily basis (Parton et al., 2007). The Grassland Ecosystem Model (GEM) (Chen et al.,
43
44
45 99 1996) linked biochemical, biophysical and ecosystem processes in a hierarchical
46
47 100 approach to simulate C and N cycles, with focus on natural grasslands. The LINGRA
48
49
50 101 model (Schapendonk et al., 1998) has been extensively applied to simulate growth of
51
52
53 102 grasses, including perennial ryegrass (Rodriguez et al., 1999) and timothy (van Oijen
54
55 103 et al., 2005) under northern and western European conditions. The Hurley Pasture
56
57
58 104 Model (Thornley, 1998) describes the fluxes of C, N and water in a grazed
59
60 105 soil-pasture-atmosphere system. DairyMod was designed to simulate not only

1
2
3
4
5 106 biophysical, but also dairy management options (Johnson et al., 2008). Several
6
7 107 integrated or whole farm system models were also available to simulate the
8
9 108 biogeochemical processes and also include decision support system, such as Whole
10
11 109 Farm Model (Bright et al., 2000), GP-FARM (Ascough et al., 2007), Integrated Farm
12
13 110 System Model (<http://www.ars.usda.gov/Main/docs.htm?docid=8519>) and FASSET
14
15 111 (Chirinda et al., 2011). An overview of the state of the art and the developments
16
17 112 needed for process-based modelling of grazed agricultural systems were addressed by
18
19 113 Snow et al. (2014).
20
21 114 Recently, attempts have also been made to introduce management options into global
22
23 115 dynamic vegetation and crop models in order to extend functionalities for grasslands
24
25 116 on regional and global scales. Biome and global dynamic vegetation models such as
26
27 117 LPJmL (Bondeau et al., 2007), Biome-BGC (Hidy et al., 2012), ORCHIDEE (Krinner
28
29 118 et al., 2005) and CARAIB (Warnant et al., 1994) were improved with mowing and
30
31 119 grazing options. At the same time, widely used crop models, such as STICS (Brisson
32
33 120 et al., 2003; Ruget et al., 2009), EPIC (Williams et al., 1989), CropSyst (Stöckle et al.,
34
35 121 2003), DNDC (Rafique et al., 2011; Wang et al., 2012), DSSAT (Giraldo et al., 1999)
36
37 122 and the APSIM platform (Holzworth et al., 2014) have also been adapted to simulate
38
39 123 grasslands. These efforts have made great contributions to the overall development of
40
41 124 grassland models (yet with a different detail in representing processes). However,
42
43 125 model evaluation was limited in scope to specific goals (e.g. not all grassland models
44
45 126 simulate biogeochemical cycles). A detailed evaluation of model performance against
46
47 127 observational flux data from a variety of grassland sites is therefore desirable. In
48
49
50
51
52
53
54
55
56
57
58
59
60
61
62
63
64
65

1
2
3
4
5 128 particular, for a process-based model representing in detail the mechanisms driving
6
7 129 the functioning of grassland systems, evaluation is needed with extended datasets,
8
9
10 130 which include different grassland observational sites with a diversity of climatic,
11
12 131 management and soil conditions.

13
14
15 132 The process-based biogeochemical Pasture Simulation model (PaSim) is the focus of
16
17 133 this study. It was originally developed by Riedo et al. (1998), based on the Hurley
18
19
20 134 Pasture Model (Thornley, 1998), to simulate managed grasslands (clover-ryegrass
21
22 135 swards). PaSim includes both grazing and cutting management options and is able to
23
24
25 136 simulate a variety of temperate grassland ecosystems. Over the last decade, the model
26
27
28 137 has been continuously improved to simulate C, water and N cycles. New approaches
29
30 138 were integrated into the modelling structure to simulate, for instance, nitrous oxide
31
32
33 139 (N₂O) emissions from soils (Schmid et al., 2001a) and methane (CH₄) emissions from
34
35 140 animals (Vuichard et al., 2007a) as well as the performances (i.e. milk and meat
36
37 141 production) of grazing animals (Graux et al., 2011). The model has been used in the
38
39
40 142 climate-change impact studies (Graux et al., 2013; Vital et al., 2013), including an
41
42 143 assessment of the contribution of forage-based systems to the global warming (Graux
43
44 144 et al., 2012) with focus on France. However, PaSim has only been evaluated against a
45
46
47 145 few European grassland sites using short periods of observed C fluxes and biomass
48
49 146 production data, and based on limited parameterization (Vuichard et al., 2007a;
50
51 147 Calanca et al., 2007). A full documentation and an extended evaluation of the model
52
53
54 148 over a large number of sites are required.

55
56
57
58
59 149 A monitoring network consisting of a total of 12 grassland sites was established in
60
61

1
2
3
4
5 150 2002 and eddy-covariance flux measurements were made on this network within the
6
7
8 151 European projects of the 5th, 6th and 7th framework programs, such as GREENGRASS
9
10 152 (Soussana et al., 2007b), CARBOMONT (Bahn et al., 2008; Wohlfahrt et al., 2008),
11
12 153 CarboEurope (Gilmanov et al., 2010) and CARBO-Extreme (Reichstein et al., 2013).
14
15 154 This dataset provides a good opportunity to evaluate grassland model performances
16
17 155 because these sites cover a variety of grassland types with contrasting management
18
19 156 practices and representing different climate conditions.
20
21
22 157 The present study assesses the ability of PaSim to reproduce C and water fluxes of a
23
24 158 number of European long-term eddy flux measurement sites. To do so, three sets of
25
26 159 eco-physiological vegetation parameters (i.e. from permanent grassland, sown
27
28 160 grassland, and an adjusted set, which is the calibrated parameter values based on flux
29
30 161 measurements data and their plausible ranges) were applied in order to test whether a
31
32 162 common set of vegetation parameters is appropriate to represent model outputs at
33
34 163 European scale (regardless of the possible physiological dissimilarities among
35
36 164 grasslands species in different places in Europe). Model calibration was not applied
37
38 165 separately to each observational site. This did not make it possible to explore the
39
40 166 spatial variability of model parameters. Testing such a scenario appeared beyond the
41
42 167 scope of this paper since it implied too strong a deviation from the initial hypothesis
43
44 168 of this regional study. Rather, we calibrated the model simultaneously on all datasets
45
46 169 to find parameter values that would be applicable at regional scale. Multi-site
47
48 170 calibration can be characterized by lower uncertainty than site-specific calibration,
49
50 171 because more data are involved in the calibration process (e.g. Minunno et al., 2014).
51
52
53
54
55
56
57
58
59
60
61
62
63
64
65

1
2
3
4
5 172 The availability of a variety of detailed flux data from multiple sites offers the
6
7
8 173 possibility of a genuine multi-location calibration of the model, holding to the
9
10 174 assumption that a uniform calibration across sites is appropriate under these
11
12 175 conditions. The results are discussed with respect to the strengths and weaknesses of
13
14
15 176 the model in estimating C and water balances in Europe before presenting conclusions
16
17
18 177 and avenues for future research.
19
20 178

179 **2. Materials and Methods**

180

181 **2.1 Study sites and climate data**

182 Twelve grassland sites with long-term eddy flux measurements were included in the
183 study to evaluate model performances. The study sites cover a broad gradient of
184 geographic and climatic conditions (Table 1) as well as a variety of soil types and
185 management practices (Table 2). The sites are located in Central and Western Europe
186 (Fig. 1, left), distributed over a range of latitudes from United Kingdom (Easter Bush)
187 to Portugal (Mitra), of longitudes from Ireland (Dripsey) to Hungary (Bugac-Puszta),
188 and of elevations from sea level up to mountain sites located at about 1800 m a.s.l.
189 (Table 1). Along these ranges, the mean annual temperature varies from 5.2 (Monte
190 Bondone, Italy) to 14.3 °C (Mitra, Portugal) with mean annual precipitation rates
191 from 520 (Bugac-Puszta, Hungary) to 1271 mm (Dripsey, Ireland). With respect to
192 management, the dataset covers the gradient from semi-natural to intensively
193 managed mixed grass species swards (in the presence of clover) and essentially
194 includes vegetation types representative of the zone. Semi-natural grasslands are
195 typified by extensive systems either grazed (with a stocking rate of ~0.5-1.0 LSU ha⁻¹
196 yr⁻¹) or not grazed (where forage production is limited to one cutting per year).
197 Otherwise, the other sites are intensively managed by grazing and/or cutting and are
198 supplied with relative large amounts of N fertilizer (>200 kg N ha⁻¹). It should be
199 noted that the distinction between extensive and intensive grasslands may not be
200 clear-cut. For instance, the unfertilized site of Amplero, grazed by a limited number of
201 livestock units (0.5 LSU ha⁻¹ yr⁻¹), qualifies as an intensive production system because

1
2
3
4
5 202 it is grazed for a long period of time in the year (200 days), with intensive utilization
6
7
8 203 of the sward and gain of N from returns by animals. At Easter Bush, the low impact of
9
10 204 grazing pressure (in number of animals and duration) is instead compatible with an
11
12 205 extensive system because the N fertilization treatment does not exceed the threshold
13
14 206 ($>200 \text{ kg N ha}^{-1}$) conventionally set for intensively managed grasslands (e.g. Bos et
15
16
17 207 al., 2005).

18
19
20 208 Monthly and yearly summaries for the average temperature and total precipitation
21
22 209 were obtained from the hourly weather data available for each site. The yearly
23
24 210 reference evapotranspiration (ET_0 , mm) was also calculated, using the
25
26 211 Penman–Monteith method, which uses an hourly time step (Allen, 2005). These
27
28 212 weather summaries were the basis for calculating two bioclimatic indicators.

29
30
31 213 The aridity pattern (Fig. 1, right) is characterized by semi-arid to humid conditions,
32
33 214 with the average value of De Martonne-Gottmann index (b) ranging from 10-20 at
34
35 215 Mitra (Portugal) and Bugac-Pusztá (Hungary) to 45 at Dripsey (Ireland). The climate
36
37 216 of Mitra is typically warm and dry for a large part of the year, with hot summers.
38
39 217 Bugac-Pusztá represents a continental climate, with hot summers, rain showers and
40
41 218 mildly cold winters. The site is characterized by annual water deficit, as well as the
42
43 219 Mediterranean upland site of Amplerò (Central Italy). The other sites are mostly
44
45 220 humid, with values of the aridity index around 30-50.
46
47
48
49
50
51
52
53

54 221

55 222 **2.2 Flux measurements**

56
57
58
59 223 Each study site was equipped with an eddy covariance system to determine the net
60
61

1
2
3
4
5 224 ecosystem exchange (NEE) of CO₂. For each site, details of the materials and
6
7 225 software used are provided by published papers (Table 1). The eddy covariance
8
9
10 226 system consisted of a fast response 3D sonic anemometer coupled with fast CO₂-H₂O
11
12 227 analyzers measuring fluxes of CO₂, latent and sensible heat, and momentum fluxes
13
14
15 228 every 30 minutes. The flux data used in this study were downloaded from the
16
17 229 European Fluxes Database Cluster (<http://www.europe-fluxdata.eu>). These data,
18
19
20 230 previously filtered(quality checking and gap-filling) using methods based on friction
21
22 231 velocity (u* filtering), contain inherent uncertainty (as detected by bootstrapping
23
24
25 232 approach, after Reichstein et al., 2005 and Papale et al., 2006). We acknowledge that
26
27
28 233 the random and systematic errors of eddy flux measurements could induce uncertainty
29
30 234 and affect interpretation of data when eddy flux data were used for model calibration
31
32
33 235 and validation (Lasslop et al., 2008). Random errors caused by poor measurement and
34
35
36 236 sampling variability can be quite large at half-hourly time resolution, while systematic
37
38 237 errors (biases) can be corrected (Aubinet et al., 2012). It is known that the correction
39
40
41 238 can be insufficient to avoid propagation of uncertainties in the gap-filling procedure
42
43
44 239 and in the partitioning of C exchanges into assimilation and respiration (Richardson et
45
46 240 al., 2012). However, the absolute uncertainty in half-hourly measurements is reduced
47
48
49 241 (down to ~10%) with daily or higher (monthly to annual) timescales and often equals
50
51
52 242 the inter-annual variability of the measured fluxes (Hagen et al., 2006; Desai et al.,
53
54 243 2008; Kroon et al., 2009).

55
56
57 244

58
59 **2.3 Model description**
60
61

Version preprint

1
2
3
4
5 246 The Pasture Simulation model (PaSim, version 5.3,
6
7 247 <https://www1.clermont.inra.fr/urep/modeles/pasim.htm>) simulates C and N cycling in
8
9 248 grassland ecosystems (mixed swards) at a sub-daily time step. The model has evolved
10
11 249 over time, starting as a simulator of dry matter production and associated flows of C,
12
13 250 N and water in productive pastures (Riedo et al., 1998). The biological N fixation by
14
15 251 clover is simulated by assuming that clover fraction in the sward is fixed for the
16
17 252 specific location (after Riedo et al., 1998). PaSim was later improved by Schmid et al.
18
19 253 (2001b) with respect to the production and diffusion of N₂O (Riedo et al., 2002) the
20
21 254 exchange of NH₃ with the atmosphere by Vuichard et al. (2007a, b), the animal
22
23 255 herbage selection and intake, and the effects of diet quality on the emissions of CH₄
24
25 256 from grazing animals. More recently, Graux et al. (2011) further improved
26
27 257 functionalities to estimate the forage production and dry matter intake taking into
28
29 258 account selective grazing between vegetation compartments and the effect of high
30
31 259 temperatures on animals, while also simulating ruminant performance and enteric
32
33 260 CH₄ emissions during grazing according to the energy content of the intake. The
34
35 261 livestock system considers change in body weight of the grazing livestock and
36
37 262 simulates the level of milk and meat production with heifers, dairy and suckler cows
38
39 263 during the grazing period.
40
41 264 The model consists of five interacting modules: microclimate, soil, vegetation,
42
43 265 herbivores and management. The soil biophysical module simulates soil temperature
44
45 266 and moisture profiles for different soil layers based on soil physical properties and
46
47 267 hourly weather inputs and simulated plant water use. The soil biogeochemical module,
48
49
50
51
52
53
54
55
56
57
58
59
60
61
62
63
64
65

1
2
3
4
5 268 adapted by monthly time-step CENTURY's organic decomposition approach (Parton,
6
7 269 1988), evenly distributes litter into the whole soil profile. The litter is segregated into
8
9
10 270 its structural and substrate components, respectively supplying the structural and
11
12 271 metabolic soil pools. In addition, the soil organic matter is further separated into three
13
14
15 272 compartments (active, slow and passive) according to different decomposition rates.
16
17 273 Soil pools are interlinked to represent C and N first-order kinetics. The N cycle
18
19
20 274 considers N inputs to the soil via atmospheric deposition, fertilizer addition, symbiotic
21
22 275 fixation by legumes and animal faeces and urine. The inorganic soil N is available for
23
24
25 276 root uptake and is lost through the processes (leaching, volatilization and
26
27 277 nitrification/denitrification) leading to N₂O and N₂ emissions to the atmosphere. The
28
29 278 vegetation module estimates the assimilated C by photosynthesis and allocates it
30
31 279 dynamically to one root and three shoot compartments, each of which consisting of
32
33 280 four age classes. The transition from one age category to the next is done using
34
35 281 threshold time values to calculate the age of biomass in a compartment from the input
36
37 282 of younger material and the loss of older material. C losses from the system are
38
39 283 through animal milking, enteric CH₄ emissions and from animal returns, and
40
41 284 ecosystem respiration. Accumulated aboveground biomass is either cut or grazed, or
42
43 285 enters a pool after senescing. Herbivores are considered during the time they were at
44
45 286 pasture (not during indoor periods). Management includes organic and mineral N
46
47 287 fertilizations, mowing and grazing, setting by the user or optimized within the model
48
49 288 to achieve some objectives.
50
51
52
53
54
55
56
57
58
59 289

1
2
3
4
5 290 **2.4 Parameterization and Simulation**
6

7 291

8
9
10 292 **2.4.1 Parameterization strategies**
11

12 293 In previous studies (Calanca et al., 2007; Vuichard et al., 2007b), PaSim was

13
14 294 evaluated for a temporary grassland at Oensingen (Switzerland) and an upland

15
16
17 295 permanent grassland at Laqueuille (France) based on a set of 26 parameters (Table 3).

18
19
20 296 We assumed that a common set of eco-physiological model parameters can be

21
22
23 297 established to simulate C₃ grasslands (including grasses, forbs and legumes) under

24
25
26 298 contrasting climate and management regimes in Europe, while site-specific climate

27
28
29 299 and management conditions provide supplementary factors driving the actual

30
31 300 production of grasslands. Based on the set of parameters given in Table 3 and

32
33
34 301 sensitivity analysis results (Ben Touhami et al., 2013), the following two steps were

35
36 302 carried out to explore the parameter space and identify a common set of

37
38
39 303 eco-physiological model parameters for PaSim. First, the model was run at all sites

40
41 304 with two sets of default parameter values: temporary sown grassland (P_temp) and

42
43
44 305 upland permanent grassland (P_perm). Second, manual calibration was carried out for

45
46 306 these parameters, which were identified as influential parameters by Ben Touhami et

47
48
49 307 al. (2013). The values of some of these parameters were modified within their

50
51
52 308 plausible ranges (as from the published literature, documented by Graux, 2011) to

53
54 309 ensure realistic representation of a variety of outputs. The calibration work was

55
56
57 310 performed at all study sites together through a trial-and-error process comparing the

58
59 311 model predictions with observational data. The solutions obtained constitute a

1
2
3
4
5 312 satisfactory performance for all output variables according to the metrics of Table 4.
6
7 313 Even though optimization methods are available (Trudinger et al., 2007; Wang et al.,
8
9 314 2009), the manual calibration is useful for modellers to get a reference parameter set
10
11 315 reflecting expert knowledge and simple adjustment strategies. It was proven that
12
13 316 optimization methods may be problematic in confronting the interaction between
14
15 317 parameters of complex models (Hollinger and Richardson, 2005; Richardson et al.,
16
17 318 2010). The model performance was evaluated for each site separately and with all
18
19 319 sites combined, by comparing the simulated C and water fluxes with data from eddy
20
21 320 flux towers.
22
23
24
25
26
27
28
29
30
31

322 **2.4.2 Model simulation and evaluation**

323 For each site, simulations were carried out with three sets of parameter values
34
35 324 described above for all available years in each site
36
37
38 325 PaSim was initialized via a spin-up process using the current weather input. In
39
40 326 particular, soil C pools were initialized to steady-state by running the model over 100
41
42 327 years by looping the available meteorology at each site following Lardy et al. (2011).
43
44 328 The results of the spin-up process matched the supplied soil C measurements with a
45
46 329 relative error of about 10% on average ($\pm \sim 2\%$ standard error).
47
48
49
50
51 330 The agreement of model outputs against the following five plant and soil variables
52
53 331 was examined, gross primary productivity (GPP, $\text{kg C m}^{-2} \text{d}^{-1}$), ecosystem respiration
54
55 332 (RECO, $\text{kg C m}^{-2} \text{d}^{-1}$), net ecosystem exchange (NEE, $\text{kg C m}^{-2} \text{d}^{-1}$), soil water content
56
57 333 ($\text{m}^3 \text{m}^{-3}$) and actual evapotranspiration (ET, mm d^{-1}). Ecosystem respiration (RECO)
58
59
60
61
62
63
64
65

1
2
3
4
5 334 plays an important role in estimating global C balances of terrestrial ecosystems, and
6
7 335 its knowledge is required to assess the GPP of such ecosystem (as a sum of NEE, and
8
9
10 336 RECO, equations in appendixes A, B, C and D). Soil water content (SWC) and soil
11
12 337 temperature (ST) were estimated for each of the six layers that make up the soil
13
14
15 338 profile in PaSim (equations in appendixes E and F).
16
17 339 Different performance indices and threshold criteria (Bennett et al., 2013) were used
18
19
20 340 to evaluate the model (Table 4). In particular, the goodness-of-fit R^2 (coefficient of
21
22 341 determination) was calculated to assess the linear dependence between modelled and
23
24
25 342 observed data and the variance explained by the model. The modelling efficiency
26
27 343 (ME), the index of agreement (IA) and the root mean square error (RMSE) were
28
29 344 derived to assess quantitative differences. The mean bias (MB) is a measure of the
30
31 345 overall tendency of the model to under- or over-estimate (the systematic error) the
32
33 346 observations. The performance of the model was assessed on daily, weekly and
34
35
36 347 monthly time scales.
37
38
39
40 348

1
2
3
4
5 **349 3. Results**

6
7
8 350 This section first describes the study sites. Then, the comparison between PaSim
9
10 351 results obtained with three sets of parameter values (two previously established and
11
12 352 one established in this study) and observed C and water fluxes is illustrated. The
13
14
15 353 model improvement gained with the new parameterization is presented. As well, the
16
17
18 354 impact of both site-specific characteristics and management options on model
19
20 355 performances is illustrated, followed by a detailed analysis of the model performances
21
22 356 with focus on C and water balances. Only exemplary results (selected output variables
23
24
25 357 and sites) are reported graphically and the main outcomes discussed hereafter, while
26
27 358 the full set of results is provided online supplementary material.

28
29
30
31 359

32
33 **360 3.1 The improvement of the model performance with the redefined parameter**
34
35 **361 values**

36
37
38 362 The adjusted parameters (denoted P_{new}) essentially reflect that previously used at
39
40
41 363 the permanent grassland site of Laqueuille (P_{perm}) (Table 3). This indicates that
42
43
44 364 Laqueuille site resembles the European grasslands used in this study, with the
45
46 365 exception of four parameters: light-saturated leaf photosynthetic rate for reproductive
47
48
49 366 stage, light-saturated leaf photosynthetic rate for vegetative stage, maximum specific
50
51
52 367 leaf area, and temperature dependence factor of the soil respiration. Even though a
53
54 368 formal sensitivity analysis was not undertaken in this study, these parameters had a
55
56 369 significant impact on model outputs in a previous study (Ben Touhami et al., 2013).

57
58
59 370 For three parameters, the new values lie between those in the previous studies. For the
60
61

1
2
3
4
5 371 parameter governing soil respiration, previous modelling studies supported a default
6
7 372 value equal to 2, which was substantially decreased (down to 0.7) to obtain simulated
8
9
10 373 respiration values closer to observations. Given its impact on the modelled RECO,
11
12 374 characterization of this parameter will require further studies.

13
14
15 375 The estimation of GPP and RECO was improved (Fig. 2) with the redefined common
16
17 376 set of eco-physiological parameters (Table 3). GPP was overestimated at all sites
18
19 377 using the P_temp parameter set with the exception of Oensingen (the site where that
20
21 378 parameter set was originally derived) and, to a lesser extent, of Amplero. Using
22
23 379 P_perm parameter set (permanent grassland), the bias of GPP was reduced at seven
24
25 380 out of 12 sites. Applying the redefined P_redif parameter set (Table 3), the bias of
26
27 381 GPP was further reduced for most of the sites except Oensingen, Bugac-Pusztza and
28
29 382 Amplero (Fig. 2).

30
31
32
33 383 With both P_temp and P_perm parameter sets, RECO was overestimated for most of
34
35 384 the sites, with the exception of Oensingen and Amplero (Fig. 2). With P_perm, a
36
37 385 slight underestimation was also obtained at intensively-managed Laqueuille (Fig. 2).
38
39 386 When the redefined parameter set was used, the bias of RECO was reduced at all sites
40
41 387 but Oensingen and Amplero. Overall, the estimated ET has a good agreement with the
42
43 388 observed values with no real improvement with the redefined parameter values (Fig. 2
44
45 389 and Fig. A1).

46
47
48
49
50
51
52
53
54 390

55
56 391 **3.2 The site variability of model performances with the redefined parameter**
57
58
59 392 **values**

1
2
3
4
5 393 Model performance in predicting GPP, RECO and ET (data aggregated on a weekly
6
7 394 basis) is closely linked with site-specific conditions such as soil moisture (e.g. dry
8
9 395 sandy soils versus humid soils). The model simulated well GPP and RECO for nine
10
11 396 out of 12 sites. The exceptions were the sites of Amplero, Mitra and Bugac-Puszt
12
13 397 (Fig. 3, Fig. 4 and Table 5), which are characterized by drier conditions than the other
14
15 398 sites. The R^2 for the estimated versus observed GPP was greater than 0.8 for most of
16
17 399 the sites and was lower than 0.5 at Amplero only ($R^2=0.40$) (Fig. 3). Similar results
18
19 400 were found when other indices, such as the slope of the regression, IA, ME and
20
21 401 RMSE were taken into account (Table. 5). Compared with GPP estimations, similar
22
23 402 model performances were found for RECO across sites, but R^2 values for RECO were
24
25 403 relatively lower than those obtained when simulating GPP. For RECO, R^2 values were
26
27 404 generally greater than 0.7 for most of the sites, but lower than 0.5 at Amplero
28
29 405 ($R^2=0.39$) and Mitra ($R^2=0.46$) (Fig. 4). At Oensingen, the model underestimated
30
31 406 RECO during winter time and there were also periods (e.g. 2007) when summer
32
33 407 modelled RECO was below of that measured (Fig. 5). However, winter RECO
34
35 408 underestimation was common to most of the sites (online supplementary material).
36
37 409 The model performance was satisfactory for predicting ET at most of the sites.
38
39 410 Exceptions were dry sites such as Amplero, Bugac-Puszt and Mitra (Fig. A1).
40
41
42
43
44
45
46
47
48
49
50
51
52
53
54
55
56
57
58
59
60
61
62
63
64
65

411

412 **3.3 The impact of site characteristics and management practices**

413 Site characteristics and management practices were observed to have an important
414 impact on the model ability to estimate RECO (Fig. 6), but they were less important

1
2
3
4
5 415 when predicting GPP, NEE, ET, and soil temperature (data not shown). Concerning
6
7 416 management practices, the model tended to underestimate or overestimate RECO,
8
9 417 respectively for intensively and extensively managed grasslands (Fig. 6). The
10
11 418 occurrence of cutting or grazing had no significant impact on the model performance
12
13 419 in predicting RECO. The model tended to slightly underestimate RECO for
14
15 420 temporary-sown grasslands, while simulations of permanent grasslands were in good
16
17 421 agreement with measured data (Fig. 6). Concerning site-specific conditions, RECO
18
19 422 was underestimated for non-montane grasslands (<800 m a.s.l.) and overestimated for
20
21 423 mountain sites (Fig. 6).

22
23
24
25
26
27
28 424 An analysis of the normalized residuals (where each residual is the difference between the
29
30 425 predicted and observed values divided by the standard deviation) showed seasonal patterns, which
31
32 426 differed by site (Fig. 7). On average, the model slightly underestimated weekly-aggregated RECO
33
34 427 in winter in most sites, but significantly overestimated it in summer time on Laqueuille extensive,
35
36 428 Monte Bondone, Alinya, Bugac-Pusztta, and Cabauw (Fig. 7). However, most of the residuals fall
37
38 429 within the upper limit of the 95% confidence interval.
39
40
41
42
43
44
45

430

46 **3.4 C and water balances**

47
48 432 The mean annual C fluxes (NEE, GPP and RECO) are meant as a synthesis and a
49
50 433 complement to the model performances of PaSim presented in this study. They
51
52 434 showed a good agreement with observations using the redefined parameter set (Fig. 8).
53
54 435 With these parameter values, the estimated NEE flux was on average $213 \text{ g C m}^{-2} \text{ yr}^{-1}$,
55
56 436 which indicates a sink of C approaching the average NEE flux observed at the studied
57
58
59
60
61
62
63
64
65

1
2
3
4 437 sites ($185 \text{ g C m}^{-2} \text{ yr}^{-1}$) (Fig. 8). The estimated yearly average values of GPP (1220 g
5
6
7 438 $\text{C m}^{-2} \text{ yr}^{-1}$) and RECO ($1006 \text{ g C m}^{-2} \text{ yr}^{-1}$) are in agreement with the observed mean
8
9
10 439 values ($1230 \text{ g C m}^{-2} \text{ yr}^{-1}$ for GPP and $1046 \text{ g C m}^{-2} \text{ yr}^{-1}$ for RECO) across all sites
11
12 440 (Fig. 8). As a consequence, the model overestimated the C sink by 15%. This is
13
14
15 441 mainly due to RECO, which is underestimated while GPP is in good agreement with
16
17 442 observations. The average value of simulated ET (415 mm yr^{-1}) for all sites and years
18
19
20 443 was close to the average value of the observations (451 mm yr^{-1}), which corresponded
21
22
23 444 to an underestimation by 8% (Fig. 9).
24
25
26 445

1
2
3
4
5 446 **4. Discussion**

6
7 447

8
9
10 448 **4.1 Model performance over European grasslands**

11
12 449 By evaluating PaSim at a variety of European sites, an improvement of model
13
14 450 performances was obtained with using a common set of parameter values to estimate
15
16 451 C and water fluxes at weekly and yearly time scales (Fig. 2, Fig. 8 and Table 3). The
17
18 452 discrepancy between the observed and estimated GPP and RECO values was reduced
19
20 453 compared with previous studies making us of parameter values obtained at specific
21
22 454 conditions (Calanca et al., 2007; Ciais et al., 2010). For instance, Calanca et al. (2007)
23
24 455 overestimated GPP of about 50% at Laqueuille (France).
25
26
27

28 456

29
30
31
32
33 457 **4.2 The spatial variability of the model performance**

34
35 458 The agreement between the observed and estimated GPP on arid sites (Bugac-Puszta,
36
37 459 Amplero) is not as good as on other sites (Fig. 3). The mismatch between observed
38
39 460 and estimated GPP values on these dry sites can be partially attributed to the fact that
40
41 461 the model did not simulate soil water content fluctuations during summer time well
42
43 462 (see effect of drought conditions for Bugac-Puszta, Fig. 2A and Amplero, Italy, Fig
44
45 463 A3). Previous studies confirmed that extreme drought events may have a significant
46
47 464 effect on C and water cycles (Ciais et al., 2005; Hussain et al., 2011). With all the
48
49 465 slope coefficients less than 1, the range of the simulated soil water content was
50
51 466 smaller than the observed range, while the intercept was well above 0 (Fig. A4),
52
53 467 indicating that the model overestimated the soil water content during dry periods and
54
55
56
57
58
59
60
61
62

1
2
3
4
5 468 underestimated it the rest of time. As a consequence, the overestimated soil water
6
7 469 content during drought periods could explain the slight overestimation of GPP (Fig.
8
9
10 470 A2). In contrast, at Mitra (Portugal), the underestimated GPP can be partially
11
12 471 attributed to the underestimated soil water content during the growing season (Fig. A5)
13
14
15 472 as water is the limitation factor of plant growth in arid regions. Underestimation of
16
17 473 GPP was also obtained at Amplero (Italy), but the incomplete information available
18
19
20 474 for this site (Fig. A3) about starting and ending dates of grazing (constant dates were
21
22
23 475 used) makes interpretation of results difficult.

24
25 476 Comparing with GPP, a similar model performance for RECO was found, but R^2 for
26
27 477 RECO is relatively lower than GPP (Fig. 3). The lower R^2 for RECO on most of the
28
29
30 478 sites is mainly due to the underestimated RECO during winter as, for instance, at
31
32
33 479 Bugac-Puszta (Fig.7, A2). On one hand the underestimated RECO during winter can
34
35
36 480 be attributed to underestimation of soil temperature in the same period as soil
37
38 481 respiration is sensitive to temperature. Soil respiration, one of the main components of
39
40
41 482 RECO, depends on soil moisture, clay content, soil organic matter and C assimilation
42
43
44 483 (Bahn et al., 2008; Balogh et al., 2011; Migliavacca et al., 2011) and these are also the
45
46 484 drivers of PaSim. On another hand, the overestimated RECO at Bugac-Puszta is
47
48
49 485 partially due to overestimated GPP as more C substrate is available. A third reason
50
51
52 486 might be that the model overestimated soil moisture content (Fig. A2 and Fig. A5)
53
54 487 since soil moisture is one of the most important limiting factors of soil respiration
55
56 488 especially in arid and semi-arid regions (Balogh et al., 2011). At Amplero and Mitra,
57
58
59 489 RECO underestimation follows GPP underestimation (Fig. A3 and Fig. A5). Indeed,

1
2
3
4
5 490 RECO is intimately related to C supply (Bahn et al., 2008; Migliavacca et al., 2011).
6
7
8 491

9
10 492 **4.3 Effect of site-specific conditions and management practices**
11

12 493 Management practices affect grassland production and greenhouse gas emissions
13
14 494 from grassland systems (Schmitt et al., 2010; Zeeman et al., 2010; Luo et al., 2012;
15
16 495 Peichl et al., 2012). In this study, PaSim underestimated RECO for
17
18 496 intensively-managed grasslands such as Oensingen and Amplero and overestimated it
19
20 497 for extensively-managed grasslands (Fig. 6, 7). It is known that intensive management
21
22 498 practices can introduce pronounced changes to soil physical structure, which in turn
23
24 499 impact the soil water transport processes and the soil heterotrophic respiration
25
26 500 (Moyano et al., 2012; Ball, 2013). It is the case for the present study as PaSim did not
27
28 501 simulate adequately soil water fluctuations (Fig. 5, Fig. A2 and Fig. A3). At
29
30 502 Oensingen (Switzerland), the model did not represent well the soil temperature (Fig. 5.
31
32 503 This can be mainly attributed to the disturbance of management, which changed the
33
34 504 soil structure when converting cropland into grassland at Oensingen in 2001,
35
36 505 considering that tillage changes soil physical structure and, in turn, water and energy
37
38 506 transport processes (Acharya et al., 2012). The human management could also modify
39
40 507 microbial component and diversity (Cantarel et al., 2012), which significantly impacts
41
42 508 on the soil respiration (Allison et al., 2010; Wieder et al., 2013). Moreover, the
43
44 509 possibility to introduce more uncertainties is high due to imprecise input management
45
46 510 information such as grazing, cutting, and fertilization rate and timing.
47
48
49
50
51
52
53
54
55
56
57
58
59 511

1
2
3
4
512 **4.4 Limitations and further improvement**

513 Referring to the model performance discussed above, certain modules of PaSim were
514 identified as worthy of further development. One is the soil energy balance module
515 because the model underestimated soil temperature when air temperature was high in
516 summer (Fig. A5) and overestimated soil temperature in winter when air temperature
517 is low (Fig. 5, Fig. A2, Fig. A3 and Fig. A5). The soil water transport module is also
518 critical because soil water fluctuations were not well captured by the model (Fig. 5,
519 Fig. A2, Fig. A3 and Fig. A5), especially on arid and semi-arid grasslands. Moreover,
520 the effect of standing biomass on the energy balance (with shading and albedo) has
521 not been investigated.

522 The choice of eco-physiological parameters used and calibrated manually in this study
523 also requires a forma quantification of the parameter uncertainties introduced in
524 regional studies. The interaction between model parameters is also an issue. For
525 example, specific leaf area (*sla*), which depends on the maximum value set for it
526 (*slam*), interacts in PaSim with C allocation-parameters across different organs of the
527 plant. A higher *sla* could induce a lower allocation of assimilated C to leaf, which may
528 be not the case in reality.

529

1
2
3
4 530 **5. Conclusions and perspectives**

5
6 531

7 532 **5.1 Summary of findings of the regional-scale analysis**

8
9
10 533 A regional-scale analysis of C and water cycles was performed on a variety of
11
12 534 European grassland sites using a process-based model (PaSim) with a single set of
13
14
15 535 eco-physiological parameters. It was shown that: 1) variables of C and water cycles
16
17 536 (mainly GPP, RECO and ET) can be reasonably simulated by PaSim at European
18
19
20 537 scale using a common set of parameter values; 2) better model performances are
21
22
23 538 obtained at more humid sites; 3) RECO tends to be underestimated in
24
25
26 539 intensively-managed grasslands and overestimated at sites when extensive
27
28 540 management practices are adopted.

29
30
31 541 The parameterization for mechanistic simulation of grasslands (with biogeochemical
32
33 542 capabilities) is a general way to facing regional studies. We have pursued in this study
34
35
36 543 the question of to what extent calibration can improve the parameterization of a
37
38
39 544 complex grassland model for regional-scale simulations in Europe. Acting upon the
40
41
42 545 most influential parameters of PaSim, we have derived a set of parameter values of
43
44 546 general validity in Europe. Even if for specific purposes process-based models need to
45
46 547 be parameterized on a site-specific basis, our multi-dataset procedure demonstrates
47
48
49 548 that it is possible to find global estimates for those parameters that encompass a wide
50
51
52 549 range of conditions. The accurate estimation of C and water fluxes relies on the
53
54 550 mechanistic representation of key ecosystem processes, with parameters that can be
55
56
57 551 related to physical quantities, thus the perspective of using a regionally calibrated
58
59 552 model regulating energy and matter exchanges is more interesting than applying

1
2
3
4
5 553 statistical models (Laniak et al., 2013). In addition, statistical model estimations may
6
7 554 involve significant levels of collinearity among predictor variables such as
8
9 555 temperature and precipitation. They also rely on the assumption of stationarity (e.g.
10
11 556 assuming that past relationships will hold in the future, even if factors such as climate
12
13 557 and management evolve) and are subject to problems of low signal-to-noise ratios in
14
15 558 yield or weather records in many locations (Lobell and Burke, 2010). The main
16
17 559 finding is that the satisfactory performance obtained over contrasting climate
18
19 560 conditions and management options justify the use of PaSim in regional studies on C
20
21 561 and water fluxes in Europe. In C-water flux studies, this is especially relevant when
22
23 562 daily-resolution outputs are mainly analysed in temporally-aggregated form - that is,
24
25 563 the interest is in weekly, monthly or higher timeframes (e.g. Wallach and Thorburn,
26
27 564 2014).

28
29
30
31
32
33
34
35
36
37
38 566 **5.2 Future work on grassland modelling**

39
40
41 567 Our results indicate further model development is needed to address specific needs
42
43 568 and this is critical under the pressure of a changing climate and related extreme
44
45 569 weather events, potentially altering the C cycles at different scales (Field et al., 2011).
46
47 570 A first issue is that heat waves and dry spells have (favouring conditions of aridity) a
48
49 571 direct effect on CO₂ fluxes because warmer temperatures and soil moisture shortage
50
51 572 affect both photosynthesis and respiration. Moreover, as changes in seasonal water
52
53 573 availability have pronounced effects on individual species, a prominent role is
54
55 574 suggested for species interactions in ecosystem responses to climate changes (Suttle et

Version preprint

1
2
3
4
5 575 al., 2007). Adaptation and functional biodiversity would dampen down the effect of
6
7 576 climate extremes on the C cycle, but the bases for biological adaptation and the role of
8
9
10 577 biodiversity are still unclear (Reichstein et al., 2013b). The use of functional traits of
11
12 578 plants, for which plant species are classified into functional types based on vegetative
13
14
15 579 and reproductive traits, proposed by Cruz et al. (2002) can be a promising avenue for
16
17
18 580 future research (Duru et al., 2013). But the level of detail of this study is too low to
19
20
21 581 draw conclusions about the relationship between model parameters and phenotypic
22
23 582 traits.

24
25 583 To obtain reliable estimates of the sign (source or sink) and magnitude of C-cycle
26
27
28 584 feedbacks, future research should provide a mechanistic basis for inferring effects of
29
30
31 585 extreme meteorological events on the C cycle. This would also help capturing the
32
33 586 impacts of drought events on grasslands because drought avoidance of grassland
34
35
36 587 plants mainly depends on rooting depth and soil water reserves. Concepts by Baker et
37
38 588 al. (2008) and Sheikh et al. (2009), which consider root access to the stored water in
39
40
41 589 the deep soil water during the drought season, could be integrated into PaSim.

42
43 590 The soil temperature module is another area of the model to be improved to better
44
45
46 591 predict soil temperature over winter. This is especially critical for high-altitude
47
48
49 592 grasslands, where vegetative growth restarts at snowmelt. This would also improve
50
51
52 593 the estimation of soil respiration, for which soil temperature is a key driver.

53
54 594 Moreover, we acknowledge that the dynamics of aboveground biomass accumulation
55
56
57 595 (either cut for yield production or grazed by animals) were not considered in the study
58
59 596 design. Biomass data are mostly discontinuously measured and rather large

1
2
3
4
5 597 uncertainties on biomass measurements (mainly owing to spatial heterogeneity) may
6
7
8 598 hinder model evaluation (Vuichard, 2007b). A better model performance (yet
9
10 599 integrating biomass measurements) could be attained by optimizing model parameters
11
12 600 through model-data fusion methods such as Bayesian calibration (van Oijen et al.,
13
14
15 601 2011). Studies of this type are underway on PaSim (Ben Touhami et al., 2012a, b)
16
17 602 with attention given to the interaction among parameters.

18
19
20 603 The improvements of PaSim also include the development of scalable solutions with
21
22 604 fundamental plant science research (a broad range of basic impact processes, open to
23
24
25 605 a wide range of plant types) and transition of software engineering technology into
26
27 606 modelling practice (Martin et al., 2011; Lardy et al., 2014), while addressing
28
29 607 re-usability issues and inter-linking of model components (Donatelli et al., 2012).

30
31
32
33 608 For managed grasslands, complete management information is often unavailable for
34
35
36 609 regional studies. High-quality grassland management data are needed to better
37
38 610 understand their effects on the soil physical structure and C storage (Flechard et al.,
39
40
41 611 2007; Schmitt et al., 2010; Chang et al., 2013).

42
43 612 The model improvement actions are ongoing under the guidance and conditions laid
44
45
46 613 down by a number of international projects and initiatives (e.g. AgMIP,
47
48 614 <http://www.agmip.org>), and will be expanded by the EU-FP7 project
49
50
51 615 MODEXTREME (<http://modextreme.org>).

52
53
54 616

1
2
3
4
5 617 **Acknowledgments**
6

7 618 The results of this research were obtained within an international research project
8
9 619 named “FACCE MACSUR – Modelling European Agriculture with Climate Change
10
11 620 for Food Security, a FACCE JPI knowledge hub”. The data used were obtained with
12
13 621 the support of EU projects CarboEurope-IP (FP6 GOCE-CT-2003-505572) and
14
15 622 CARBO-Extreme (FP7-ENV-2008-1-226701). We thank Partner Institutions for
16
17 623 providing grassland data. We also acknowledge technical support from the European
18
19 624 Fluxes Database Cluster (<http://www.europe-fluxdata.eu>). Several reviewers and the
20
21 625 editors helped considerably in improving the manuscript.
22

23 626
24
25
26
27
28
29
30
31
32
33
34
35
36
37
38
39
40
41
42
43
44
45
46
47
48
49
50
51
52
53
54
55
56
57
58
59
60
61
62
63

1
2
3
4 627 **APPENDICES**

5
6 628 **Appendix A - Primary production**

7
8 629 Gross primary production (GPP) is the rate at which the plant captures and stores a
9
10 630 given amount of chemical energy as biomass in a given length of time. Some fraction
11
12 631 of this fixed energy is used for cellular respiration and maintenance of existing tissues
13
14 632 (growth respiration and maintenance respiration). The remaining fixed energy (as
15
16 633 mass of photosynthate) is referred to as net primary production (NPP):

17
18 634
$$NPP = GPP - R_{pl,tot} \quad (1)$$

19
20 635 where $R_{pl,tot}$ is the total plant respiration (autotrophic).

21
22 636 Plant residues deposited to the soil are subject to biological degradation. During this
23
24 637 process, soil organic C is respired to CO₂ while providing energy to the decomposers
25
26 638 (microorganisms and soil fauna). Heterotrophic C fluxes can also include respiratory
27
28 639 losses of CO₂ by grazing ruminants. The combined autotrophic and heterotrophic
29
30 640 ecosystem respiration (RECO) is the CO₂ release from the plants ($R_{pl,tot}$), soil (R_{soil})
31
32 641 and animals (R_{an}). The ensemble of instantaneous inward and outward flows of C
33
34 642 within the ecosystem is the Net Ecosystem Exchange (NEE), given by:

35
36 643
$$NEE = RECO - GPP \quad (2)$$

37
38 644 with positive values indicating the system is a source of C losses, and negative values
39
40 645 indicating that the system sequesters C from the atmosphere.

41 646

42 647 **Appendix B - Total plant respiration**

43
44 648 A single process of respiration is associated with growth (Thornley, 1998). A
45
46 649 component of this respiratory flux is deemed to be maintenance respiration (generally
47
48 650 associated with the re-synthesis of degrading tissue), while also taking into account
49
50 651 the energy required for mineral uptake. The dependence of respiratory components on
51
52 652 C substrate supply is represented by separating C substrate from structure and
53
54 653 coupling the respiration flux to photosynthesis. This allows simulating variation in the
55
56 654 fractions of total plant respiration associated with different processes during plant
57
58 655 development.

59 656 Total plant respiration, $R_{pl,tot}$ (kg C m⁻² d⁻¹), is given by:

1
2
3
4 657 $R_{pl,tot} = R_{m,rt} + R_{m,sh} + R_{G,rt} + R_{G,sh} + R_N$ (3)
5

6 658 R_G and R_m stand for growth and maintenance respiration, respectively, referred to
7
8 659 shoot (index *sh*) and root (index *rt*). R_N is the respiratory flux associated with uptake
9
10 660 of N from the soil solution. The terms $R_{m,rt}$, $R_{G,rt}$ and R_N are soil respiratory fluxes
11
12 661 from the biological activity of roots (autotrophic soil respiration).
13

14 662

15
16 663 *Growth respiration rates*

17
18 664 The two respiration fluxes needed to produce energy for the growth of shoots and
19
20 665 roots, $R_{G,sh}$ and $R_{G,rt}$ (kg C m⁻² d⁻¹), respectively, are calculated as:

21
22 666 $R_{G,sh} = I_{C,G_{sh}} \cdot \left(\frac{1}{Y_{G,pl}} - 1 \right)$ (4)
23

24
25 667 $R_{G,rt} = I_{C,G_{rt}} \cdot \left(\frac{1}{Y_{G,pl}} - 1 \right)$ (5)
26

27 668 The term $1/Y_{G,pl}$ is an efficiency measure representing the kg of C required to create 1
28
29 669 kg of structural C, $Y_{G,pl}$ being the photosynthetically-assimilated C initially allocated
30
31 670 to substrate C reserves and then used for growth and maintenance of tissues. For the
32
33 671 fraction required for growth, growth rates (kg C m⁻² d⁻¹) are calculated for
34
35 672 aboveground ($I_{C,G_{sh}}$) and belowground ($I_{C,G_{rt}}$) biomass, based on allocation values
36
37 673 occurring during the vegetative stage ($I_{C,G_{sh,veg}}$ and $I_{C,G_{rt,veg}}$, kg C m⁻² d⁻¹), modified in
38
39 674 favour of aboveground biomass during the reproductive stage. The coefficient $Y_{G,pl}$ is
40
41 675 set equal to 0.75 to represent plant growth efficiency (kg C (kg C)⁻¹).
42

43
44 676 C allocation fluxes into roots ($I_{C,G_{rt}}$) and aboveground ($I_{C,G_{sh}}$) plant parts are as
45
46 677 follows:
47

48 678 $I_{C,G_{rt}} = I_{C,G_{rt,veg}} - f_{devstage} \cdot I_{C,G_{rt,veg}}$ (6)
49

50 679 $I_{C,G_{sh}} = I_{C,G_{sh,veg}} + f_{devstage} \cdot I_{C,G_{rt,veg}}$ (7)
51

52 680 Where $f_{devstage}$ is a factor depending on the plant development stage.

53
54
55 681 The terms $I_{C,G_{sh,veg}}$ and $I_{C,G_{rt,veg}}$ are calculated on a constant growth rate at 20 °C ($I_{C,G20}$,
56
57 682 usually set equal to 150 kg² (kg C)⁻¹ (kg N)⁻¹), applied to the cumulative structural
58
59 683 biomass of roots and shoots (W_{sh} , W_{rt} , kg DM m⁻²) and modulated by factors of
60

684 temperature ($f_{T,G}$) and substrate C and N concentrations in shoots and roots (C_{sh} , C_{rt} ,
 685 kg C (kg DM)⁻¹; N_{sh} , N_{rt} , kg N (kg DM)⁻¹), as follows:

$$686 \quad I_{C,G_{sh,veg}} = I_{C,G20} \cdot f_{T,G} \cdot C_{sh} \cdot N_{sh} \cdot W_{sh} \quad (8)$$

$$687 \quad I_{C,G_{rt,veg}} = I_{C,G20} \cdot f_{T,G} \cdot C_{rt} \cdot N_{rt} \cdot W_{rt} \quad (9)$$

688
 689 *Maintenance respiration rates*

690 The respiration fluxes to maintain metabolic processes (those that do not result in a
 691 net increase in plant dry matter) of roots ($R_{m,rt}$) and shoots ($R_{m,sh}$) are a function of
 692 substrate C concentration (C , kg C kg DM⁻¹), structural biomass ($W_{sh} \cdot f_{C,sh}$, $W_{rt} \cdot f_{C,rt}$)
 693 and a temperature-dependent stress factor (Table 3):

$$694 \quad R_{m,sh} = \frac{C}{C + K_{C,mai}} \cdot R_{m,sh,temp} \quad (10)$$

$$695 \quad R_{m,rt} = \frac{C}{C + K_{C,mai}} \cdot R_{m,rt,temp} \quad (11)$$

696 where $K_{C,mai}$ is a maintenance respiration parameter, set equal to 0.03 kg substrate C
 697 (kg structural DM)⁻¹ d⁻¹. The terms $R_{m,sh,temp}$ and $R_{m,rt,temp}$ are temporary shoot and root
 698 maintenance respiration, respectively, as follows:

$$699 \quad R_{m,sh,temp} = f_{T,sh} \cdot \sum_{j=1}^4 k_{mai,j,20} \cdot W_{sh,j} \cdot f_{C,sh} \quad (12)$$

$$700 \quad R_{m,rt,temp} = f_{T,rt} \cdot \sum_{j=1}^4 k_{mai,j,20} \cdot W_{rt,j} \cdot f_{C,rt} \quad (13)$$

701 These maintenance respiration factors are transient in nature since they apply to
 702 temporary values. Both shoot and root biomasses are indeed divided into four state
 703 variables representing four age categories ($j=1, \dots, 4$), for which the following values
 704 are given for the maintenance respiration parameter at 20 °C, $k_{mai,j,20}$ (kg C
 705 kg⁻¹ structural C d⁻¹): 0.020 ($j=1$), 0.020 ($j=2$), 0.015 ($j=3$), 0.010 ($j=4$).

706 The terms $f_{C,sh}$ and $f_{C,rt}$ (kg C kg⁻¹ DM) are fractional C content in shoot and root
 707 structural dry matter, respectively (reference values are 0.50 and 0.39, respectively).

708
 709 *N uptake respiration rate*

710 The respiration flux associated with N uptake (R_N , kg C m⁻² d⁻¹) is:

$$711 \quad R_N = k_N \cdot IN_{soil,rt} \quad (14)$$

712 where $IN_{soil,rt}$ (kg Nm⁻²) is the mineral N (NO₃⁻-N and NH₄⁺-N) uptake by the sward,

1
2
3
4 and k_N is the respiratory cost of N uptake (the reference value being $0.45 \text{ kg C kg}^{-1} \text{ N}$).
5
6

7
8
9
10
11
12
13
14
15
16
17
18
19
20
21
22
23
24
25
26
27
28
29
30
31
32
33
34
35
36
37
38
39
40
41
42
43
44
45
46
47
48
49
50
51
52
53
54
55
56
57
58
59
60
61
62
63
64
65

715 **Appendix C – Heterotrophic soil respiration**

716 Apart the biological activity of roots and associated micro-organisms, the flux of CO_2
717 from the soil to the atmosphere is the result of the production of CO_2 from the activity
718 of heterotrophic bacteria and fungi living on litter and in the root-free soil (after
719 Parton, 1988). The soil organic carbon (SOC) pool is divided into five pools with
720 different turnover times ranging from 0.5 to 1500 years. An additional component is
721 given by the amount of C released as exudates (*exu*) from roots into the soil, estimated
722 as a fraction of plant substrate C. The litter in decomposition over the total soil depth
723 splits into its structural and substrate components, supplying the structural (*str*) and
724 metabolic (*met*) soil pools respectively. Other three compartments with different
725 decomposition rates include active (*act*), slow (*slo*) and passive (*pas*) pools of SOC,
726 consisting of the microbial biomass, refractory components of litter and highly
727 humified organic compounds respectively.

728 Total heterotrophic soil respiration, R_{SOC} ($\text{kg C m}^{-2} \text{ d}^{-1}$), is given by:

$$729 R_{SOC} = R_{str} + R_{met} + R_{exu} + R_{act} + R_{slo} + R_{pas} \quad (15)$$

731 *Soil respiration from structural organic matter*

732 The respiration flux associated with structural SOC (R_{str} , $\text{kg C m}^{-2} \text{ d}^{-1}$) is:

$$733 R_{str} = (1 - f_{lig, str}) \cdot f_{r, str} \cdot f_{C, str} + f_{lig, str} \cdot f_{r, str, lig} \cdot f_{C, str} \quad (16)$$

734 The microbial respiration parameter for the decomposition of the structural pool, $f_{r, str}$,
735 and of lignin, $f_{r, str, lig}$, are set equal to 0.55 and 0.3, respectively. The term $f_{lig, str}$ is the
736 fraction of lignin in structural soil organic matter. The fraction of C in the structural
737 plant residue, $f_{C, str}$, is as follows:

$$738 f_{C, str} = k_{str} \cdot W_{C, str} \quad (17)$$

739 where k_{str} ($\text{kg C m}^{-2} \text{ d}^{-1}$) is the decomposition rate for the structural pool and $W_{C, str}$ (kg
740 C m^{-2}) is the C content in structural fraction of plant residue (depending on
741 temperature, lignin, texture and water content).
742

1
2
3
4 743 *Soil respiration from metabolic organic matter*

5
6 744 The respiration flux associated with metabolic SOC (R_{met} , kg C m⁻²d⁻¹) is:

7
8 745 $R_{met} = f_{r,met} \cdot f_{C,met}$ (18)

9
10 746 The microbial respiration parameter for the decomposition of the metabolic pool, $f_{r,met}$,
11 747 is set equal to 0.55. The fraction of C in metabolic pool, $f_{C,met}$ (kg C m⁻²), is calculated
12 748 assuming linear kinetics.

13
14
15
16 749
17
18 750 *Soil respiration from exudates*

19
20 751 The respiration flux associated with root exudates (R_{exu} , kg C m⁻² d⁻¹) is:

21
22 752 $R_{exu} = f_{r,exu} \cdot f_{C,exu}$ (19)

23
24 753 The parameter $f_{r,exu}$ is set equal to 0.75. The term $f_{C,exu}$ (kg C m⁻²) is C substrate output
25 754 for root exudation.

26
27
28 755
29
30 756 *Soil respiration from active organic matter*

31
32 757 The respiration flux associated with active SOC (R_{act} , kg C m⁻²d⁻¹) is:

33
34 758 $R_{act} = f_{r,act} \cdot f_{C,act}$ (20)

35
36 759 The fraction of C in active pool, $f_{C,act}$ (kg C m⁻²), is calculated as follows:

37
38 760 $f_{r,act} = 0.85 - 0.68 \cdot (f_{clay,ah} + f_{silt,ah})$ (21)

39
40 761 where f_{clay} and f_{silt} are fractions of clay and silt, respectively.

41
42
43 762
44 763 *Soil respiration from slow organic matter*

45
46 764 The respiration flux associated with slow SOC (R_{slo} , kg C m⁻²d⁻¹) is:

47
48 765 $R_{slo} = f_{r,slo} \cdot f_{C,slo}$ (22)

49
50 766 The microbial respiration parameter for the decomposition of the slow pool, $f_{r,slo}$, is set
51 767 equal to 0.55. The fraction of C in slow fraction, $f_{C,met}$ (kg C m⁻²), is calculated as
52 768 follows.

53
54
55 769 $f_{r,slo} = k_{slo} \cdot W_{C,slo}$ (23)

56
57 770 $k_{slo} = k_{slo,20} \cdot k_{dec,t} \cdot k_{dec,\theta}$ (24)

58
59 771 $W_{C,slo}$ (kg C m⁻²) is the C content in slow pool (depending on temperature, lignin,
60 772 texture and water content). The term $k_{slo,20}$ (d⁻¹) is the turnover rate for slow C pool at

1
2
3
4 773 20 °C, equal to 0.00027. The terms $k_{dec,t}$ and $k_{dec,\theta}$ are factor activities of soil organic
5
6 774 matter for temperature and water content, respectively.

7
8 775

9
10 776 *Soil respiration from passive organic matter*

11 777 The respiration flux associated with active SOC (R_{pas} , kg C m⁻²d⁻¹) is:

12
13
14 778 $R_{pas} = f_{r,pas} \cdot f_{C,pas}$ (25)

15 779 The microbial respiration parameter for the decomposition of the passive pool, $f_{r,pas}$, is
16
17 780 set equal to 0.55. The fraction of C in passive pool, $f_{C,pas}$ (kg C m⁻²), is calculated
18
19 781 assuming linear kinetics.

20
21
22 782

23
24 783 **Appendix D - Respiration from grazing animals**

25 784 Half of the C in plant material consumed by grazing animals ($I_{C,veg\rightarrow ani}$, kg C m⁻² d⁻¹)
26
27 785 is assumed to be respired (R_{ani} , kg C m⁻²d⁻¹):

28
29
30 786 $R_{ani} = 0.5 \cdot I_{C,veg\rightarrow ani}$ (26)

31 787 The amount of ingested C is estimated as follows:

32
33
34 788 $I_{C,veg\rightarrow ani} = (f_{C,sh} + C) \cdot \frac{W_{sh}}{W_{sh,tot}} \cdot I_{veg\rightarrow ani}$ (27)

35
36 789 where ($I_{veg\rightarrow ani}$, kg DM m⁻² d⁻¹) is the amount of ingested dry matter, which increases
37
38 790 with the aboveground plant biomass ($W_{sh,tot}$, kg DM m⁻²) available for the animals
39
40 791 (W_{sh} , kg DM m⁻², is the cumulative structural aboveground biomass), limited by the
41
42 792 maximum ingestion capacity the animal is able to maintain (I_{max} , whose reference
43
44 793 value is 16 kg DM d⁻¹ animal⁻¹).

45
46 794

1
2
3
4 **795 Appendix E - Soil temperature**

5
6 796 The calculation of temperature in each soil layer is based on the energy balance
7
8 797 equations for the different soil layers (Campbell, 1985; Monteith, 1965; Shuttleworth
9
10 798 and Wallace, 1985):

11
12 799 $T_s^*(h) = 0.6 \cdot T_s(h) + (1 - 0.6) \cdot T_s'(h)$ (28)
13

14 800 Where $T_s(h)$ (K) is the soil temperature at the midpoint of the i^{th} layer in the present
15
16 801 time step, $T_s'(h)$ (K) is soil temperature in the same layer but one time step in the past,
17
18 802 and $T_s^*(h)$ (K) is temperature in the i^{th} layer at some time between the two time steps.
19

20
21 803 **Appendix F - Soil water balance**

22 804 The water content in the different soil layers determines photosynthesis and stomatal
23
24 805 conductance, soil evaporation, and rates of soil biological processes, and is used to
25
26 806 calculate soil temperature in the different layers, which influences belowground plant
27
28 807 processes, soil heat flux, and soil biological processes. Values of the soil matrix
29
30 808 potential in soil layer h , $\psi(h)$ (m), is related to the water content in the same layer,
31
32 809 $\theta_s(h)$ ($\text{m}^3 \text{m}^{-3}$) by the soil moisture characteristic (Campbell, 1985):
33

34
35 811 $\theta_s(h) = \theta_{s,sat}(h) \cdot \left[\frac{\psi_e(h)}{\psi(h)} \right]^{\frac{1}{b(h)}}$ (29)
36

37 812 where $\theta_{s,sat}(h)$ ($\text{m}^3 \text{m}^{-3}$) is the saturation soil water content in soil layer h , $\psi_e(h)$ is the
38
39 813 air entry water potential (m) in soil layer h , $b(h)$ is a physical parameter for soil layer
40
41 814 h .

1
2
3
4 **815 References**
5

- 6 816 Acharya, B.S., Rasmussen, J., Eriksen, J., 2012. Grassland carbon sequestration and emissions
7 817 following cultivation in a mixed crop rotation. *Agriculture, Ecosystems & Environment*
8 818 153, 33–39. doi:10.1016/j.agee.2012.03.001
9
10 819 Addiscott, T.M., Whitmore, A.P., 1987. Computer simulation of changes in soil mineral nitrogen
11 820 and crop nitrogen during autumn, winter and spring. *The Journal of Agricultural Science*
12 821 109, 141-157. doi:10.1017/S0021859600081089
13
14 822 Aires, L.M.I., Pio, C.A., Pereira, J.S., 2008. Carbon dioxide exchange above a Mediterranean C3/C4
15 823 grassland during two climatologically contrasting years. *Global Change Biology* 14,
16 824 539–555. doi:10.1111/j.1365-2486.2007.01507.x
17
18 825 Allen, R.G., Walter, I.A., Elliot, R.L., Howell, T.A., Itenfisu, D., Jensen, M.E., Snyder, R., 2005. The
19 826 ASCE standardized reference evapotranspiration equation. American Society of Civil
20 827 Engineers, Reston.
21
22 828 Allison, S.D., Wallenstein, M.D., Bradford, M.A., 2010. Soil-carbon response to warming
23 829 dependent on microbial physiology. *Nature Geoscience* 3, 336–340.
24 830 doi:10.1038/ngeo846
25
26 831 Ammann, C., Flechard, C.R., Leifeld, J., Neftel, A., Fuhrer, J., 2007. The carbon budget of newly
27 832 established temperate grassland depends on management intensity. *Agriculture,*
28 833 *Ecosystems & Environment* 121, 5–20. doi:10.1016/j.agee.2006.12.002
29
30 834 Ascough, J.C., McMaster, G.S., Andales, A.A., Hansen, N.C., Sherrrod, L.A., 2007. Evaluating
31 835 GPFARM crop growth, soil water and soil nitrogen components for Colorado dryland
32 836 locations. *Transactions of the ASABE* 50, 1565–1578.
33
34 837 Aubinet, M., Vesala, T., Papale, D., 2012. Eddy covariance: A practical guide to measurement and
35 838 data analysis. Springer, Dordrecht.
36
37 839 Bahn, M., Rodeghiero, M., Anderson-Dunn, M., Dore, S., Gimeno, C., Droesler, M., Williams, M.,
38 840 Ammann, C., Berninger, F., Flechard, C., Jones, S., Balzarolo, M., Kumar, S., Newesely, C.,
39 841 Priwitzer, T., Raschi, A., Siegwolf, R., Susiluoto, S., Tenhunen, J., Wohlfahrt, G., Cernusca,
40 842 A., 2008. Soil respiration in European grasslands in relation to climate and assimilate
41 843 supply. *Ecosystems* 11, 1352–1367. doi:10.1007/s10021-008-9198-0
42
43 844 Baker, I.T., Prihodko, L., Denning, A.S., Goulden, M., Miller, S., da Rocha, H.R., 2008. Seasonal
44 845 drought stress in the Amazon: Reconciling models and observations. *Journal of*
45 846 *Geophysical Research* 113, G00B01. doi:10.1029/2007JG000644
46
47 847 Ball, B.C., 2013. Soil structure and greenhouse gas emissions: a synthesis of 20 years of
48 848 experimentation. *European Journal of Soil Science* 64, 357–373. doi:10.1111/ejss.12013
49
50 849 Balogh, J., Pintér, K., Fóti, S., Cserhalmi, D., Papp, M., Nagy, Z., 2011. Dependence of soil
51 850 respiration on soil moisture, clay content, soil organic matter, and CO₂ uptake in dry
52 851 grasslands. *Soil Biology and Biochemistry* 43, 1006–1013.
53 852 doi:10.1016/j.soilbio.2011.01.017
54
55 853 Ben Touhami, H., Lardy, R., Barra, V., 2012a. Bayesian calibration of the Pasture Simulation Model
56 854 (PaSim) to simulate European grasslands under climate extremes: case study at Stubai
57 855 (Austria). 11th PSAM & ESREL Conference, 25-29 June, Helsinki, Finland, 1, 567-577.
58
59 856 Ben Touhami, H., Lardy, R., Gilgen, A., Buchmann, N., Bellocchi, G., 2012b. Bayesian calibration of
60 857 the Pasture Simulation Model (PaSim) to simulate Swiss grasslands under climate
61 858 extremes. 12th Congress of the European Society for Agronomy, 20-24 August, Helsinki,

- 1
2
3
4 859 Finland, 441-5.
5 860 Ben Touhami, H.B., Lardy, R., Barra, V., Bellocchi, G., 2013. Screening parameters in the Pasture
6 861 Simulation model using the Morris method. *Ecological Modelling* 266, 42–57.
7 862 doi:10.1016/j.ecolmodel.2013.07.005
8
9 863 Bennett, N.D., Croke, B.F.W., Guariso, G., Guillaume, J.H.A., Hamilton, S.H., Jakeman, A.J.,
10 864 Marsili-Libelli, S., Newham, L.T.H., Norton, J.P., Perrin, C., Pierce, S.A., Robson, B., Seppelt,
11 865 R., Voinov, A.A., Fath, B.D., Andreassian, V., 2013. Characterising performance of
12 866 environmental models. *Environmental Modelling & Software* 40, 1–20.
13 867 doi:10.1016/j.envsoft.2012.09.011
14
15 868 Bondeau, A., Kicklighter, D.W., Kaduk, J., The Participants of the Potsdam NdP Model
16 869 intercomparison, 1999. Comparing global models of terrestrial net primary productivity
17 870 (NPP): importance of vegetation structure on seasonal NPP estimates. *Global Change*
18 871 *Biology* 5, 35–45. doi:10.1046/j.1365-2486.1999.00005.x
19
20 872 Bondeau, A., Smith, P.C., Zaehle, S., Schaphoff, S., Lucht, W., Cramer, W., Gerten, D., 2007.
21 873 Modelling the role of agriculture for the 20th century global terrestrial carbon balance.
22 874 *Global Change Biology* 13, 679–706. doi:10.1111/j.1365-2486.2006.01305.x
23
24 875 Bos, J.F.F., Pflimlin, A., Aarts, H.F.M., Vertès, F., 2005. Nutrient management at farm scale. How to
25 876 attain policy objectives in regions with intensive dairy farming? *Plant Research*
26 877 *International Report* 83, Plant Research International, Wageningen, 260 pp.
27
28 878 Bright, K.P., Sherlock, R.A., Lile, J., Wastney, M.E., 2000. Development and use of a whole farm
29 879 model for dairying. In: Halloy, S., Williams, T. (Eds.), *Applied complexity - from neural*
30 880 *nets to managed landscapes*. NZ Institute for Crop and Food Research, Christchurch, pp.
31 881 382-389.
32
33 882 Brisson, N., Gary, C., Justes, E., Roche, R., Mary, B., Ripoche, D., Zimmer, D., Sierra, J., Bertuzzi, P.,
34 883 Burger, P., 2003. An overview of the crop model STICS. *European Journal of Agronomy* 18,
35 884 309–332. doi:10.1016/S1161-0301(02)00110-7
36
37 885 Butler, M.P., Davis, K.J., Denning, A.S., Kawa, S.R., 2010. Using continental observations in global
38 886 atmospheric inversions of CO₂: North American carbon sources and sinks. *Tellus B* 62,
39 887 550–572. doi:10.1111/j.1600-0889.2010.00501.x
40
41 888 Byrne, K.A., Kiely, G., 2006. Partitioning of Respiration in an Intensively Managed Grassland. *Plant*
42 889 *and Soil* 282, 281–289. doi:10.1007/s11104-005-6065-z
43
44 890 Calanca, P., Vuichard, N., Campbell, C., Viovy, N., Cozic, A., Fuhrer, J., Soussana, J.F., 2007.
45 891 Simulating the fluxes of CO₂ and N₂O in European grasslands with the Pasture Simulation
46 892 Model (PaSim). *Agriculture Ecosystems & Environment* 121, 164–174. doi:
47 893 10.1016/j.agee.2006.12.010
48
49 894 Campbell, G.S., 1985. *Soil physics with BASIC: transport models for soil-plant systems*. Elsevier,
50 895 Amsterdam.
51
52 896 Cantarel, A.A.M., Bloor, J.M.G., Pommier, T., Guillaumaud, N., Moirot, C., Soussana, J.-F., Poly, F.,
53 897 2012. Four years of experimental climate change modifies the microbial drivers of N₂O
54 898 fluxes in an upland grassland ecosystem. *Global Change Biology* 18, 2520–2531.
55 899 doi:10.1111/j.1365-2486.2012.02692.x
56
57 900 Chang, J., Viovy, N., Vuichard, N., Ciais, P., Wang, T., Cozic, A., Lardy, R., Graux, A.-I., Klumpp, K.,
58 901 Martin, R., Soussana, J.-F., 2013. Incorporating grassland management in a global
59 902 vegetation model: model description and evaluation at 11 eddy-covariance sites in

- 1
2
3
4 903 Europe. Geoscientific Model Development Discussions 6, 2769–2812.
5 904 doi:10.5194/gmdd-6-2769-2013
- 6
7 905 Chen, D.-X., Hunt, H.W., Morgan, J.A., 1996. Responses of a C3 and C4 perennial grass to CO₂
8 906 enrichment and climate change: Comparison between model predictions and
9 907 experimental data. Ecological Modelling 87, 11–27. doi:10.1016/0304-3800(94)00199-5
- 10
11 908 Chirinda, N., Kracher, D., Lægdsmand, M., Porter, J.R., Olesen, J.E., Petersen, B.M., Doltra, J., Kiese,
12 909 R., Butterbach-Bahl, K., 2011. Simulating soil N₂O emissions and heterotrophic CO₂
13 910 respiration in arable systems using FASSET and MoBiLE-DNDC. Plant and Soil 343,
14 911 139–160. doi:10.1007/s11104-010-0596-7
- 15
16 912 Churkina, G., Running, S.W., Schloss, A.L., The Participants of the Potsdam NdP Model
17 913 intercomparison, 1999. Comparing global models of terrestrial net primary productivity
18 914 (NPP): the importance of water availability. Global Change Biology 5, 46–55.
19 915 doi:10.1046/j.1365-2486.1999.00006.x
- 20
21 916 Ciais, P., Reichstein, M., Viovy, N., Granier, A., Ogée, J., Allard, V., Aubinet, M., Buchmann, N.,
22 917 Bernhofer, C., Carrara, A., Chevallier, F., De Noblet, N., Friend, A.D., Friedlingstein, P.,
23 918 Grünwald, T., Heinesch, B., Keronen, P., Knohl, A., Krinner, G., Loustau, D., Manca, G.,
24 919 Matteucci, G., Miglietta, F., Ourcival, J.M., Papale, D., Pilegaard, K., Rambal, S., Seufert, G.,
25 920 Soussana, J.F., Sanz, M.J., Schulze, E.D., Vesala, T., Valentini, R., 2005. Europe-wide
26 921 reduction in primary productivity caused by the heat and drought in 2003. Nature 437,
27 922 529–533. doi:10.1038/nature03972
- 28
29 923 Ciais, P., Sabine, C., Bala, G., Bopp, L., Brovkin, V., Canadell, J., Chhabra, A., DeFries, R., Galloway,
30 924 J., Heimann, M., Jones, C., Le Quéré, C., Myneni, R.B., Piao S., Thornton, P., 2013. Carbon
31 925 and other biogeochemical cycles. In: Stocker, T.F., Qin, D., Plattner, G.-K., Tignor, M., Allen,
32 926 S.K., Boschung, J., Nauels, A., Xia, Y., Bex, V., Midgley, P.M. (Eds.), Climate Change 2013:
33 927 The Physical Science Basis. Contribution of Working Group I to the Fifth Assessment
34 928 Report of the Intergovernmental Panel on Climate Change. Cambridge University Press,
35 929 Cambridge, pp. 465-570. <<http://www.ipcc.ch/report/ar5/wg1>>
- 36
37 930 Ciais, P., Soussana, J.F., Vuichard, N., Luysaert, S., Don, A., Janssens, I.A., Piao, S.L., Dechow, R.,
38 931 Lathièrre, J., Maignan, F., Wattenbach, M., Smith, P., Ammann, C., Freibauer, A., Schulze,
39 932 E.D., the CARBOEUROPE Synthesis Team, 2010. The greenhouse gas balance of
40 933 European grasslands. Biogeosciences Discussions 7, 5997–6050.
41 934 doi:10.5194/bgd-7-5997-2010
- 42
43 935 De Jager, J.M., 1994. Accuracy of vegetation evaporation ratio formulae for estimating final wheat
44 936 yield. Water SA 20, 307–314.
- 45
46 937 De Martonne, E, 1942. Nouvelle carte mondiale de l'indice d'aridité. Annales de Géographie 51,
47 938 242-250 (in French).
- 48
49 939 Desai, A.R., Richardson, A.D., Moffat, A.M., Kattge, J., Hollinger, D.Y., Barr, A., Falge, E., Noormets,
50 940 A., Papale, D., Reichstein, M., Stauch, V.J., 2008. Cross-site evaluation of eddy covariance
51 941 GPP and RE decomposition techniques. Agricultural and Forest Meteorology 148,
52 942 821-838. doi:10.1016/j.agrformet.2007.11.012
- 53
54 943 Diodato, N., Ceccarelli, M., 2004. Multivariate indicator Kriging approach using a GIS to classify
55 944 soil degradation for Mediterranean agricultural lands. Ecological Indicators 4, 177–187.
56 945 doi:10.1016/j.ecolind.2004.03.002
- 57
58 946 Donatelli, M., Cerrani, I., Fanchini, D., Fumagalli, D., Rizzoli, A.E., 2012. Enhancing model reuse via

- 1
2
3
4 947 component-centered modeling frameworks: the vision and example realizations. In:
5 948 Seppelt, R., Voinov, A.A., Lange, S., Bankamp, D. (Eds.), Proceedings of International
6 949 Congress on Environmental Modelling and Software Managing Resources of a Limited
7 950 Planet, Sixth Biennial Meeting, Leipzig, Germany, pp. 1185–1192.
- 9 951 Duru, M., Jouany, C., Le Roux, X., Navas, M.L., Cruz, P., 2013. From a conceptual framework to an
10 952 operational approach for managing grassland functional diversity to obtain targeted
11 953 ecosystem services: Case studies from French mountains. *Renewable Agriculture and*
12 954 *Food Systems* 23, 239–254. doi:10.1017/S1742170513000306
- 14 955 EC, 2008. Regulation (EC) No 1166/2008 of the European Parliament and of the Council of 19
15 956 November 2008 on farm structure surveys and the survey on agricultural production
16 957 methods and repealing Council Regulation (EEC). Official Journal of the European Union,
17 958 Brussels.
- 19 959 Flechard, C.R., Ambus, P., Skiba, U., Rees, R.M., Hensen, A., van Amstel, A., Dasseelaar, A. van den
20 960 P., Soussana, J.F., Jones, M., Clifton-Brown, J., Raschi, A., Horvath, L., Neftel, A., Jocher,
21 961 M., Ammann, C., Leifeld, J., Fuhrer, J., Calanca, P., Thalman, E., Pilegaard, K., Di Marco, C.,
22 962 Campbell, C., Nemitz, E., Hargreaves, K.J., Levy, P.E., Ball, B.C., Jones, S.K., van de Bulk,
23 963 W.C.M., Groot, T., Blom, M., Domingues, R., Kasper, G., Allard, V., Ceschia, E., Cellier, P.,
24 964 Laville, P., Henault, C., Bizouard, F., Abdalla, M., Williams, M., Baronti, S., Berretti, F.,
25 965 Grosz, B., 2007. Effects of climate and management intensity on nitrous oxide emissions
26 966 in grassland systems across Europe. *Agriculture, Ecosystems & Environment* 121,
27 967 135–152. doi:10.1016/j.agee.2006.12.024
- 29 968 Fox, D.G., 1981. Judging air quality model performance. *Bulletin of the American Meteorological*
30 969 *Society* 62, 599–609.
31 970 doi:http://dx.doi.org/10.1175/1520-0477(1981)062<0599:JAQMP>2.0.CO;2
- 33 971 Gilmanov, T.G., Aires, L., Barcza, Z., Baron, V.S., Belelli, L., Beringer, J., Billesbach, D., Bonal, D.,
34 972 Bradford, J., Ceschia, E., Cook, D., Corradi, C., Frank, A., Gianelle, D., Gimeno, C.,
35 973 Gruenwald, T., Guo, H., Hanan, N., Haszpra, L., Heilman, J., Jacobs, A., Jones, M.B.,
36 974 Johnson, D.A., Kiely, G., Li, S., Magliulo, V., Moors, E., Nagy, Z., Nasyrov, M., Owensby, C.,
37 975 Pinter, K., Pio, C., Reichstein, M., Sanz, M.J., Scott, R., Soussana, J.F., Stoy, P.C., Svejcar, T.,
38 976 Tuba, Z., Zhou, G., 2010. Productivity, respiration, and light-response parameters of
39 977 world grassland and agroecosystems derived from flux-tower measurements. *Rangeland*
40 978 *Ecology & Management* 63, 16–39. doi:10.2111/REM-D-09-00072.1
- 42 979 Giraldo, L.M., Lizcano, L.J., Gijsman, A.J., Rivera, B., Franco, L.H., 1999. Adapting the CROPGRO
43 980 model of DSSAT to simulate the growth of *Brachiaria decumbens*. In: Proceedings of The
44 981 Third International Symposium on Systems Approaches for Agricultural Development.
45 982 Lima, Peru, pp. 1–10.
- 47 983 Graux, A.-I., Bellocchi, G., Lardy, R., Soussana, J.-F., 2013. Ensemble modelling of climate change
48 984 risks and opportunities for managed grasslands in France. *Agricultural and Forest*
49 985 *Meteorology* 170, 114–131. doi:10.1016/j.agrformet.2012.06.010
- 51 986 Graux, A.I., Gaurut, M., Agabriel, J., Baumont, R., Delagarde, R., Delaby, L., Soussana, J.F., 2011.
52 987 Development of the Pasture Simulation Model for assessing livestock production under
53 988 climate change. *Agriculture, Ecosystems & Environment* 144, 69–91. doi:
54 989 10.1016/j.agee.2011.07.001
- 56 990 Graux, A.-I., Lardy, R., Bellocchi, G., Soussana, J.-F., 2012. Global warming potential of French

- 1
2
3
4 991 grassland-based dairy livestock systems under climate change. *Regional Environmental*
5 992 *Change* 12, 751–763. doi:10.1007/s10113-012-0289-2
6
7 993 Hagen, S.C., Braswell, B.H., Linder, E., Frohking, S., Richardson, A.D., Hollinger, D.Y., 2006. Statistical
8 994 uncertainty of eddy flux–based estimates of gross ecosystem carbon exchange at
9 995 Howland Forest, Maine. *Journal of Geophysical Research* 111, D08S03.
10 996 doi:10.1029/2005JD006154.
11
12 997 Hidy, D., Barcza, Z., Haszpra, L., Churkina, G., Pintér, K., Nagy, Z., 2012. Development of the
13 998 Biome-BGC model for simulation of managed herbaceous ecosystems. *Ecological*
14 999 *Modelling* 226, 99–119. doi:10.1016/j.ecolmodel.2011.11.008
15
16 1000 Hollinger, D.Y., Richardson, A.D., 2005. Uncertainty in eddy covariance measurements and its
17 1001 application to physiological models. *Tree Physiology* 25, 873–885.
18 1002 doi:10.1093/treephys/25.7.873
19
20 1003 Holzworth, D.P., Huth, N.I., deVoil, P.G., Zurcher, E.J., Herrmann, N.I., McLean, G., Chenu, K., van
21 1004 Oosterom, E., Snow, V.O., Murphy, C., Moore, A.D., Brown, H.E., Whish, J.P.M., Verrall, S.,
22 1005 Fainges, J., L.W., B., Peake, A.S., Poulton, P.L., Hochman, Z., Thorburn, P.J., Gaydon, D.S.,
23 1006 Dalgliesh, N.P., Rodriguez, D., Cox, H., Chapman, S., Doherty, A., Teixeira, E., Sharp, J.,
24 1007 Cichota, R., Vogeler, I., Li, F.Y., Wang, E., Hammer, G.L., Robertson, M.J., Dimes, J.,
25 1008 Carberry, P.S., Hargreaves, J.N.G., MacLeod, N., McDonald, C., Harsdorf, J., Wedgwood, S.,
26 1009 Keating, B.A., 2014. APSIM - Evolution towards a new generation of agricultural systems
27 1010 simulation. *Environmental Modelling & Software*, in press.
28 1011 doi:10.1016/j.envsoft.2014.07.009
29
30 1012 Huntzinger, D.N., Post, W.M., Wei, Y., Michalak, A.M., West, T.O., Jacobson, A.R., Baker, I.T., Chen,
31 1013 J.M., Davis, K.J., Hayes, D.J., Hoffman, F.M., Jain, A.K., Liu, S., McGuire, A.D., Neilson, R.P.,
32 1014 Potter, C., Poulter, B., Price, D., Raczka, B.M., Tian, H.Q., Thornton, P., Tomelleri, E., Viovy,
33 1015 N., Xiao, J., Yuan, W., Zeng, N., Zhao, M., Cook, R., 2012. North American Carbon Program
34 1016 (NACP) regional interim synthesis: Terrestrial biospheric model intercomparison.
35 1017 *Ecological Modelling* 232, 144–157. doi:10.1016/j.ecolmodel.2012.02.004
36
37 1018 Hussain, M.Z., Gruenwald, T., Tenhunen, J.D., Li, Y.L., Mirzae, H., Bernhofer, C., Otieno, D., Dinh,
38 1019 N.Q., Schmidt, M., Waringer, M., Owen, K., 2011. Summer drought influence on CO₂ and
39 1020 water fluxes of extensively managed grassland in Germany. *Agriculture, Ecosystems &*
40 1021 *Environment* 141, 67–76. doi:10.1016/j.agee.2011.02.013
41
42 1022 Jacobs, C.M.J., Jacobs, A.F.G., Bosveld, F.C., Hendriks, D.M.D., Hensen, A., Kroon, P.S., Moors, E.J.,
43 1023 Nol, L., Schrier-Uijl, A., Veenendaal, E.M., 2007. Variability of annual CO₂ exchange from
44 1024 Dutch grasslands. *Biogeosciences* 4, 803–816. doi:10.5194/bg-4-803-2007
45
46 1025 Janssens, I.A., Freibauer, A., Schlamadinger, B., Ceulemans, R., Ciais, P., Dolman, A.J., Heimann, M.,
47 1026 Nabuurs, G.-J., Smith, P., Valentini, R., 2005. The carbon budget of terrestrial ecosystems
48 1027 at country-scale – a European case study. *Biogeosciences* 2, 15–26.
49 1028 doi:10.5194/bg-2-15-2005
50
51 1029 Johnson, I.R., Chapman, D.F., Snow, V.O., Eckard, R.J., Parsons, A.J., Lambert, M.G., Cullen, B.R.,
52 1030 2008. DairyMod and EcoMod: biophysical pasture-simulation models for Australia and
53 1031 New Zealand. *Australian Journal of Experimental Agriculture* 48, 621-631.
54 1032 doi:10.1071/EA07133
55
56 1033 Jung, M., Reichstein, M., Margolis, H.A., Cescatti, A., Richardson, A.D., Arain, M.A., Arneth, A.,
57 1034 Bernhofer, C., Bonal, D., Chen, J., Gianelle, D., Gobron, N., Kiely, G., Kutsch, W., Lasslop,

- 1
2
3
4 1035 G., Law, B.E., Lindroth, A., Merbold, L., Montagnani, L., Moors, E.J., Papale, D.,
5 1036 Sottocornola, M., Vaccari, F., Williams, C., 2011. Global patterns of land-atmosphere
6 1037 fluxes of carbon dioxide, latent heat, and sensible heat derived from eddy covariance,
7 1038 satellite, and meteorological observations. *Journal of Geophysical Research* 116, G00J07.
8 1039 doi:10.1029/2010JG001566
9
10 1040 Jung, M., Vetter, M., Herold, M., Churkina, G., Reichstein, M., Zaehle, S., Ciais, P., Viovy, N.,
11 1041 Bondeau, A., Chen, Y., Trusilova, K., Feser, F., Heimann, M., 2007. Uncertainties of
12 1042 modeling gross primary productivity over Europe: A systematic study on the effects of
13 1043 using different drivers and terrestrial biosphere models. *Global Biogeochemical Cycles* 21,
14 1044 GB4021. doi:10.1029/2006GB002915
15
16 1045 Klumpp, K., Tallec, T., Guix, N., Soussana, J.-F., 2011. Long-term impacts of agricultural practices
17 1046 and climatic variability on carbon storage in a permanent pasture. *Global Change Biology*
18 1047 17, 3534–3545. doi:10.1111/j.1365-2486.2011.02490.x
19
20 1048 Krinner, G., Viovy, N., de Noblet-Ducoudré, N., Ogée, J., Polcher, J., Friedlingstein, P., Ciais, P., Sitch,
21 1049 S., Prentice, I.C., 2005. A dynamic global vegetation model for studies of the coupled
22 1050 atmosphere-biosphere system. *Global Biogeochemical Cycles* 19, GB1015.
23 1051 doi:10.1029/2003GB002199
24
25 1052 Kroon, P.S., Hensen, A., Jonker, H.J.J., Ouwensloot, H.G., Vermeulen, A.T., Bosveld, F.C., 2009.
26 1053 Uncertainties in eddy covariance flux measurements assessed from CH₄ and N₂O
27 1054 observations. *Agricultural and Forest Meteorology* 150, 806-816. doi:
28 1055 10.1016/j.agrformet.2009.08.008
29
30 1056 Laniak, G.F., Olchin, G., Goodall, J., Voinov, A., Hill, M., Glynn, P., Whelan, G., Geller, G., Quinn, N.,
31 1057 Blind, M., Peckham, S., Reaney, S., Gaber, N., Kennedy, R., Hughes, A., 2013. Integrated
32 1058 environmental modeling: A vision and roadmap for the future. *Environmental Modelling*
33 1059 & Software 39, 3–23. doi:10.1016/j.envsoft.2012.09.006
34
35 1060 Lardy, R., Bachelet, B., Bellocchi, G., Hill, D.R.C., 2014. Towards vulnerability minimization of
36 1061 grassland soil organic matter using metamodels. *Environmental Modelling & Software* 52,
37 1062 38–50. doi:10.1016/j.envsoft.2013.10.015
38
39 1063 Lasslop, G., Reichstein, M., Kattge, J., Papale, D., 2008. Influences of observation errors in eddy
40 1064 flux data on inverse model parameter estimation. *Biogeosciences* 5, 1311-1324.
41 1065 doi:doi:10.5194/bg-5-1311-2008
42
43 1066 Liu, M., He, H., Yu, G., Sun, X., Zhang, L., Han, S., Wang, H., Zhou, G., 2012. Uncertainty analysis in
44 1067 data processing on the estimation of net carbon exchanges at different forest ecosystems
45 1068 in China. *Journal of Forest Research* 17, 312–322. doi:10.1007/s10310-011-0323-0
46
47 1069 Luo, G., Han, Q., Zhou, D., Li, L., Chen, X., Li, Y., Hu, Y., Li, B.L., 2012. Moderate grazing can
48 1070 promote aboveground primary production of grassland under water stress. *Ecological*
49 1071 *Complexity* 11, 126–136. doi:10.1016/j.ecocom.2012.04.004
50
51 1072 Lobell, D.B., Burke, M.B., 2010. On the use of statistical models to predict crop yield
52 1073 responses to climate change. *Agricultural and Forest Meteorology* 150, 1443–1452.
53 1074 doi:10.1016/j.agrformet.2010.07.008
54
55 1075 Martin, G., Martin-Clouaire, R., Rellier, J.P., Duru, M., 2011. A simulation framework for the
56 1076 design of grassland-based beef-cattle farms. *Environmental Modelling & Software* 26,
57 1077 371–385. doi:10.1016/j.envsoft.2010.10.002
58
59 1078 Migliavacca, M., Reichstein, M., Richardson, A.D., Colombo, R., Sutton, M.A., Lasslop, G.,
60
61
62
63
64
65

- 1
2
3
4 1079 Tomelleri, E., Wohlfahrt, G., Carvalhais, N., Cescatti, A., Mahecha, M.D., Montagnani, L.,
5 1080 Papale, D., Zaehle, S., Arain, A., Arneth, A., Black, T.A., Carrara, A., Dore, S., Gianelle, D.,
6 1081 Helfter, C., Hollinger, D., Kutsch, W.L., Lafleur, P.M., Nouvellon, Y., Rebmann, C., Da
7 1082 ROCHA, H.R., Rodeghiero, M., Rouspard, O., Sebastià, M.-T., Seufert, G., Soussana, J.-F.,
8 1083 Van Der MOLEN, M.K., 2011. Semiempirical modeling of abiotic and biotic factors
9 1084 controlling ecosystem respiration across eddy covariance sites. *Global Change Biology* 17,
10 1085 390–409. doi:10.1111/j.1365-2486.2010.02243.x
11 1086 Minunno, F., Peltoniemi, M., Launiainen, S., Mäkelä, A., 2014. Integrating ecosystems
12 1087 measurements from multiple eddy-covariance sites to a simple model of ecosystem
13 1088 process - Are there possibilities for a uniform model calibration? *Geophysical Research*
14 1089 *Abstracts* 16, EGU2014-10706-3.
15 1090 Monteith, J., 1965. Evaporation and environment. *Symposium of the Society for Experimental*
16 1091 *Biology* 19, 205–234.
17 1092 Moriasi, D., Arnold, J., Van Liew, M., Bingner, R., Harmel, R., Veith, T., 2007. Model evaluation
18 1093 guidelines for systematic quantification of accuracy in watershed simulations.
19 1094 *Transactions of the ASABE* 50, 885–900.
20 1095 Moyano, F.E., Vasilyeva, N., Bouckaert, L., Cook, F., Craine, J., Curiel Yuste, J., Don, A., Epron, D.,
21 1096 Formanek, P., Franzluebbers, A., Ilstedt, U., Kätterer, T., Orchard, V., Reichstein, M., Rey,
22 1097 A., Ruamps, L., Subke, J.-A., Thomsen, I.K., Chenu, C., 2012. The moisture response of soil
23 1098 heterotrophic respiration: interaction with soil properties. *Biogeosciences* 9, 1173–1182.
24 1099 doi:10.5194/bg-9-1173-2012
25 1100 Nash, J.E., Sutcliffe, J.V., 1970. River flow forecasting through conceptual models part I — A
26 1101 discussion of principles. *Journal of Hydrology* 10, 282–290.
27 1102 doi:10.1016/0022-1694(70)90255-6
28 1103 Palosuo, T., Kersebaum, K.C., Angulo, C., Hlavinka, P., Moriondo, M., Olesen, J.E., Patil, R.H., Ruget,
29 1104 F., Rumbaur, C., Takac, J., Trnka, M., Bindi, M., caldag, B., Ewert, F., Ferrise, R., Mirschel,
30 1105 W., Saylan, L., Siska, B., Roeter, R., 2011. Simulation of winter wheat yield and its
31 1106 variability in different climates of Europe: A comparison of eight crop growth models.
32 1107 *European Journal of Agronomy* 35, 103–114. doi: 10.1016/j.eja.2011.05.001
33 1108 Papale, D., Reichstein, M., Aubinet, M., Canfora, E., Bernhofer, C., Longdoz, B., Kutsch, W., Rambal,
34 1109 S., Valentini, R., Vesala, T., Yakir, D., 2006. Towards a standardized processing of net
35 1110 ecosystem exchange measured with eddy covariance technique: algorithms and
36 1111 uncertainty estimation. *Biogeosciences* 3, 571-583. doi:10.5194/bg-3-571-2006
37 1112 Parton, W.J., 1988. Dynamics of C, N, P and S in grassland soils: a model. *Biogeochemistry* 5,
38 1113 109–131. doi:10.1007/BF02180320
39 1114 Parton, W.J., Morgan, J.A., Wang, G., Del Grosso, S., 2007. Projected ecosystem impact of the
40 1115 Prairie Heating and CO₂ Enrichment experiment. *New Phytologist* 174, 823–834.
41 1116 doi:10.1111/j.1469-8137.2007.02052.x
42 1117 Peichl, M., Carton, O., Kiely, G., 2012. Management and climate effects on carbon dioxide and
43 1118 energy exchanges in a maritime grassland. *Agriculture, Ecosystems & Environment* 158,
44 1119 132–146. doi:10.1016/j.agee.2012.06.001
45 1120 Pintér, K., Barcza, Z., Balogh, J., Czóbel, S., Csintalan, Z., Tuba, Z., Nagy, Z., 2008. Interannual
46 1121 variability of grasslands' carbon balance depends on soil type. *Community Ecology* 9,
47 1122 43–48. doi:10.1556/ComEc.9.2008.S.7

- 1
2
3
4 1123 Prescher, A.-K., Grünwald, T., Bernhofer, C., 2010. Land use regulates carbon budgets in eastern
5 1124 Germany: From NEE to NBP. *Agricultural and Forest Meteorology* 150, 1016–1025.
6 1125 doi:10.1016/j.agrformet.2010.03.008
7
8 1126 Rafique, R., Peichl, M., Hennessy, D., Kiely, G., 2011. Evaluating management effects on nitrous
9 1127 oxide emissions from grasslands using the process-based DeNitrification–DeComposition
10 1128 (DNDC) model. *Atmospheric Environment* 45, 6029–6039.
11 1129 doi:10.1016/j.atmosenv.2011.07.046
12
13 1130 Refsgaard, J.C., van der Sluijs, J.P., Højberg, A.L., Vanrolleghem, P.A., 2007. Uncertainty in the
14 1131 environmental modelling process – A framework and guidance. *Environmental Modelling*
15 1132 & *Software* 22, 1543–1556. doi:10.1016/j.envsoft.2007.02.004
16
17 1133 Reichstein, M., Bahn, M., Ciais, P., Frank, D., Mahecha, M.D., Seneviratne, S.I., Zscheischler, J.,
18 1134 Beer, C., Buchmann, N., Frank, D.C., Papale, D., Rammig, A., Smith, P., Thonicke, K., van
19 1135 der Velde, M., Vicca, S., Walz, A., Wattenbach, M., 2013. Climate extremes and the
20 1136 carbon cycle. *Nature* 500, 287–295. doi:10.1038/nature12350
21
22 1137 Reichstein, M., Falge, E., Baldocchi, D., Papale, D., Aubinet, M., Berbigier, P., Bernhofer, C.,
23 1138 Buchmann, N., Gilmanov, T., Granier, A., Grünwald, T., Havrankova, K., Ilvesniemi, H.,
24 1139 Janous, D., Knohl, A., Laurila, T., Lohila, A., Loustau, D., Matteucci, G., Meyers, T.,
25 1140 Miglietta, F., Ourcival, J.-M., Pumpanen, J., Rambal, S., Rotenberg, E., Sanz, M., Tenhunen,
26 1141 J., Seufert, G., Vaccari, F., Vesala, T., Yakir, D., Valentini, R., 2005. On the separation of net
27 1142 ecosystem exchange into assimilation and ecosystem respiration: review and improved
28 1143 algorithm. *Global Change Biology* 11, 1424–1439.
29 1144 doi:10.1111/j.1365-2486.2005.001002.x
30
31 1145 Richardson, A.D., Aubinet, M., Barr, A.G., Hollinger, D.Y., Ibrom, A., Lasslop, G., Reichstein, M.,
32 1146 2012, Uncertainty quantification. In: Aubinet, M., Vesala, T., Papale, D. (Eds.), *Eddy*
33 1147 *covariance - A practical guide to measurement and data analysis*. Springer, Dordrecht, pp.
34 1148 173–209.
35
36 1149 Richardson, A.D., Williams, M., Hollinger, D.Y., Moore, D.J.P., Dail, D.B., Davidson, E.A., Scott, N.A.,
37 1150 Evans, R.S., Hughes, H., Lee, J.T., Rodrigues, C., Savage, K., 2010. Estimating parameters of
38 1151 a forest ecosystem C model with measurements of stocks and fluxes as joint constraints.
39 1152 *Oecologia* 164, 25–40. doi:10.1007/s00442-010-1628-y
40
41 1153 Riedo, M., Grub, A., Rosset, M., Fuhrer, J., 1998. A pasture simulation model for dry matter
42 1154 production, and fluxes of carbon, nitrogen, water and energy. *Ecological Modelling* 105,
43 1155 141–183. doi:10.1016/S0304-3800(97)00110-5
44
45 1156 Riedo, M., Milford, C., Schmid, M., Sutton, M.A., 2002. Coupling soil-plant-atmosphere exchange
46 1157 of ammonia with ecosystem functioning in grasslands. *Ecological Modelling* 158, 83–110.
47 1158 doi:10.1016/S0304-3800(02)00169-2
48
49 1159 Rodriguez, D., Van Oijen, M., Schapendonk, A., 1999. LINGRA-CC: a sink–source model to
50 1160 simulate the impact of climate change and management on grassland productivity. *New*
51 1161 *Phytologist* 144, 359–368. doi:10.1046/j.1469-8137.1999.00521.x
52
53 1162 Rötter, R.P., Palosuo, T., Kersebaum, K.C., Angulo, C., Bindi, M., Ewert, F., Ferrise, R., Hlavinka, P.,
54 1163 Moriondo, M., Nendel, C., Olesen, J.E., Patil, R.H., Ruget, F., Takac, J., Trnka, M., 2012.
55 1164 Simulation of spring barley yield in different climatic zones of Northern and Central
56 1165 Europe: A comparison of nine crop models. *Field Crops Research* 133, 23–36.
57 1166 doi:10.1016/j.fcr.2012.03.016
58
59
60
61
62
63
64
65

- 1
2
3
4 1167 Ruget, F., Satger, S., Volaire, F., Lelièvre, F., 2009. Modeling tiller density, growth, and yield of
5 1168 Mediterranean perennial grasslands with STICS. *Crop Science* 49, 2379–2385.
6 1169 doi:doi:10.2135/cropsci2009.06.0323
7
8 1170 Schaefer, K., Schwalm, C.R., Williams, C., Arain, M.A., Barr, A., Chen, J.M., Davis, K.J., Dimitrov, D.,
9 1171 Hilton, T.W., Hollinger, D.Y., Humphreys, E., Poulter, B., Raczka, B.M., Richardson, A.D.,
10 1172 Sahoo, A., Thornton, P., Vargas, R., Verbeeck, H., Anderson, R., Baker, I., Black, T.A.,
11 1173 Bolstad, P., Chen, J., Curtis, P.S., Desai, A.R., Dietze, M., Dragoni, D., Gough, C., Grant, R.F.,
12 1174 Gu, L., Jain, A., Kucharik, C., Law, B., Liu, S., Lokipitiya, E., Margolis, H.A., Matamala, R.,
13 1175 McCaughey, J.H., Monson, R., Munger, J.W., Oechel, W., Peng, C., Price, D.T., Ricciuto, D.,
14 1176 Riley, W.J., Roulet, N., Tian, H., Tonitto, C., Torn, M., Weng, E., Zhou, X., 2012. A
15 1177 model-data comparison of gross primary productivity: Results from the North American
16 1178 Carbon Program site synthesis. *Journal of Geophysical Research* 117, G03010.
17 1179 doi:10.1029/2012JG001960
18
19 1180 Schapendonk, A.H.C.M., Stol, W., van Kraalingen, D.W.G., Bouman, B.A.M., 1998. LINGRA, a
20 1181 sink/source model to simulate grassland productivity in Europe. *European Journal of*
21 1182 *Agronomy* 9, 87–100. doi:10.1016/S1161-0301(98)00027-6
22
23 1183 Schmid, M., Fuhrer, J., Neftel, A., 2001a. Nitrous oxide concentrations in the soil of a mown
24 1184 grassland: comparison of model results with soil profile measurements. *Water, Air, & Soil*
25 1185 *Pollution: Focus* 1, 437–446. doi:10.1023/A:1013158028103
26
27 1186 Schmid, M., Neftel, A., Riedo, M., Fuhrer, J., 2001b. Process-based modelling of nitrous oxide
28 1187 emissions from different nitrogen sources in mown grassland. *Nutrient Cycling in*
29 1188 *Agroecosystems* 60, 177–187. doi:10.1023/a:1012694218748
30
31 1189 Schmitt, M., Bahn, M., Wohlfahrt, G., Tappeiner, U., Cernusca, A., 2010. Land use affects the net
32 1190 ecosystem CO₂ exchange and its components in mountain grasslands. *Biogeosciences* 7,
33 1191 2297–2309. doi:10.5194/bg-7-2297-2010
34
35 1192 Schulze, E.D., Luyssaert, S., Ciais, P., Freibauer, A., Al, I.A.J. et, Schulze, E.D., Soussana, J.F., Smith,
36 1193 P., Grace, J., Levin, I., Thiruchittampalam, B., Heimann, M., Dolman, A.J., Valentini, R.,
37 1194 Bousquet, P., Peylin, P., Peters, W., Rödenbeck, C., Etiope, G., Vuichard, N., Wattenbach,
38 1195 M., Nabuurs, G.J., Poussi, Z., Nieschulze, J., Gash, J.H., Schulze, E.D., Soussana, J.F., Smith,
39 1196 P., Grace, J., Levin, I., Thiruchittampalam, B., Heimann, M., Dolman, A.J., Valentini, R.,
40 1197 Bousquet, P., Peylin, P., Peters, W., Rödenbeck, C., Etiope, G., Vuichard, N., Wattenbach,
41 1198 M., Nabuurs, G.J., Poussi, Z., Nieschulze, J., Gash, J.H., 2009. Importance of methane and
42 1199 nitrous oxide for Europe's terrestrial greenhouse-gas balance. *Nature Geoscience* 2,
43 1200 842–850. doi:10.1038/ngeo686
44
45 1201 Scurlock, J.M.O., Hall, D.O., 1998. The global carbon sink: a grassland perspective. *Global Change*
46 1202 *Biology* 4, 229–233. doi:10.1046/j.1365-2486.1998.00151.x
47
48 1203 Sheikh, V., Visser, S., Stroosnijder, L., 2009. A simple model to predict soil moisture: Bridging
49 1204 Event and Continuous Hydrological (BEACH) modelling. *Environmental Modelling &*
50 1205 *Software* 24, 542–556. doi:10.1016/j.envsoft.2008.10.005
51
52 1206 Shuttleworth, W.J., Wallace, J.S., 1985. Evaporation from sparse crops-an energy combination
53 1207 theory. *Quarterly Journal of the Royal Meteorological Society* 111, 839–855.
54 1208 doi:10.1002/qj.49711146910
55
56 1209 Snow, V.O., Rotz, C.A., Moore, A.D., Martin-Clouaire, R., Johnson, I.R., Hutchings, N.J., Eckard, R.J.,
57 1210 2014. The challenges – and some solutions – to process-based modelling of grazed

- 1
2
3
4 1211 agricultural systems. *Environmental Modelling & Software*, 62, 420-436.
5 1212 doi:10.1016/j.envsoft.2014.03.009
6
7 1213 Soussana, J.-F., Fuhrer, J., Jones, M., Van Amstel, A., 2007. The greenhouse gas balance of
8 1214 grasslands in Europe. *Agriculture, Ecosystems & Environment* 121, 1–4.
9 1215 doi:10.1016/j.agee.2006.12.001
10 1216 Stöckle, C.O., Donatelli, M., Nelson, R., 2003. CropSyst, a cropping systems simulation model.
11 1217 *European Journal of Agronomy* 18, 289–307. doi:10.1016/S1161-0301(02)00109-0
12 1218 Suttie, J.M., Reynolds, S.G., Batello, C., 2005. Grasslands of the world. Food and Agricultural
13 1219 Organization of the United Nations, Rome.
14
15 1220 Suttle, K.B., Thomsen, M.A., Power, M.E., 2007. Species interactions reverse grassland responses
16 1221 to changing climate. *Science* 315, 640–642. doi:10.1126/science.1136401
17 1222 Thornley, J.H.M., 1998. Dynamic model of leaf photosynthesis with acclimation to light and
18 1223 nitrogen. *Annals of Botany* 81, 421–430. doi:10.1006/anbo.1997.0575
19 1224 Trudinger, C.M., Raupach, M.R., Rayner, P.J., Kattge, J., Liu, Q., Pak, B., Reichstein, M., Renzullo, L.,
20 1225 Richardson, A.D., Roxburgh, S.H., Styles, J., Wang, Y.P., Briggs, P., Barrett, D., Nikolova, S.,
21 1226 2007. OptIC project: An intercomparison of optimization techniques for parameter
22 1227 estimation in terrestrial biogeochemical models. *Journal of Geophysical Research* 112.
23 1228 doi:10.1029/2006JG000367
24 1229 Van Oijen, M., Cameron, D.R., Butterbach-Bahl, K., Farahbakhshazad, N., Jansson, P.-E., Kiese, R.,
25 1230 Rahn, K.-H., Werner, C., Yeluripati, J.B., 2011. A Bayesian framework for model calibration,
26 1231 comparison and analysis: Application to four models for the biogeochemistry of a
27 1232 Norway spruce forest. *Agricultural and Forest Meteorology* 151, 1609–1621.
28 1233 doi:10.1016/j.agrformet.2011.06.017
29 1234 Van Oijen, M., Höglind, M., Hanslin, H.M., Caldwell, N., 2005. Process-based modeling of timothy
30 1235 regrowth. *Agronomy Journal* 97, 1295-1303. doi:10.2134/agronj2004.0251
31 1236 Vital, J.-A., Gaurut, M., Lardy, R., Viovy, N., Soussana, J.-F., Bellocchi, G., Martin, R., 2013.
32 1237 High-performance computing for climate change impact studies with the Pasture
33 1238 Simulation model. *Computers and Electronics in Agriculture* 98, 131–135.
34 1239 doi:10.1016/j.compag.2013.08.004
35 1240 Vuichard, N., Ciais, P., Viovy, N., Calanca, P., Soussana, J.-F., 2007a. Estimating the greenhouse gas
36 1241 fluxes of European grasslands with a process-based model: 2. Simulations at the
37 1242 continental level. *Global Biogeochemical Cycles* 21, GB1005. doi:10.1029/2005gb002612
38 1243 Vuichard, N., Soussana, J.-F., Ciais, P., Viovy, N., Ammann, C., Calanca, P., Clifton-Brown, J., Fuhrer,
39 1244 J., Jones, M., Martin, C., 2007b. Estimating the greenhouse gas fluxes of European
40 1245 grasslands with a process-based model: 1. Model evaluation from in situ measurements.
41 1246 *Global Biogeochemical Cycles* 21, GB1004. doi:10.1029/2005gb002611
42 1247 Wallach, D., Thorburn, P.J., 2014. The error in agricultural systems model prediction depends on
43 1248 the variable being predicted. *Environmental Modelling & Software* 62, 487-494. doi:
44 1249 10.1016/j.envsoft.2014.08.001
45 1250 Wang, J., Cardenas, L.M., Misselbrook, T.H., Cuttle, S., Thorman, R.E., Li, C., 2012. Modelling
46 1251 nitrous oxide emissions from grazed grassland systems. *Environmental Pollution* 162,
47 1252 223–233. doi:10.1016/j.envpol.2011.11.027
48 1253 Wang, Y.-P., Trudinger, C.M., Enting, I.G., 2009. A review of applications of model–data fusion to
49 1254 studies of terrestrial carbon fluxes at different scales. *Agricultural and Forest*

- 1
2
3
4 1255 Meteorology 149, 1829–1842. doi:10.1016/j.agrformet.2009.07.009
5 1256 Warmink, J.J., Janssen, J.A.E.B., Booij, M.J., Krol, M.S., 2010. Identification and classification of
6 1257 uncertainties in the application of environmental models. *Environmental Modelling &*
7 1258 *Software* 25, 1518–1527. doi:10.1016/j.envsoft.2010.04.011
8
9 1259 Warnant, P., François, L., Strivay, D., Gérard, J.C., 1994. CARAIB: A global model of terrestrial
10 1260 biological productivity. *Global Biogeochemical Cycles* 8, 255–270.
11 1261 doi:10.1029/94gb00850
12
13 1262 Warszawski, L., Frieler, K., Huber, V., Piontek, F., Serdeczny, O., Schewe, J., 2014. The Inter-Sectoral
14 1263 Impact Model Intercomparison Project (ISI-MIP): Project framework. *Proceedings of the*
15 1264 *National Academy of Sciences* 111, 3228–3232. doi:10.1073/pnas.1312330110
16
17 1265 Wattenbach, M., Sus, O., Vuichard, N., Lehuger, S., Gottschalk, P., Li, L., Leip, A., Williams, M.,
18 1266 Tomelleri, E., Kutsch, W.L., Buchmann, N., Eugster, W., Dietiker, D., Aubinet, M., Ceschia,
19 1267 E., Béziat, P., Grünwald, T., Hastings, A., Osborne, B., Ciais, P., Cellier, P., Smith, P., 2010.
20 1268 The carbon balance of European croplands: A cross-site comparison of simulation
21 1269 models. *Agriculture, Ecosystems & Environment* 139,
22 1270 419–453. doi:10.1016/j.agee.2010.08.004
23
24 1271 Wieder, W.R., Bonan, G.B., Allison, S.D., 2013. Global soil carbon projections are improved by
25 1272 modelling microbial processes. *Nature Climate Change* 3, 909-912.
26 1273 doi:10.1038/nclimate1951
27
28 1274 Williams, J.R., Jones, C.A., Kiniry, J.R., Spanel, D.A., 1989. The EPIC crop growth model.
29 1275 *Transactions of the ASAE* 32, 497-511. doi:10.13031/2013.31032
30
31 1276 Willmott, C.J., Wicks, D.E., 1980. An Empirical Method for the Spatial Interpolation of Monthly
32 1277 Precipitation within California. *Physical Geography* 1, 59–73.
33 1278 doi:10.1080/02723646.1980.10642189
34
35 1279 Wohlfahrt, G., Anderson-Dunn, M., Bahn, M., Balzarolo, M., Berninger, F., Campbell, C., Carrara,
36 1280 A., Cescatti, A., Christensen, T., Dore, S., Eugster, W., Friborg, T., Furger, M., Gianelle, D.,
37 1281 Gimeno, C., Hargreaves, K., Hari, P., Haslwanter, A., Johansson, T., Marcolla, B., Milford, C.,
38 1282 Nagy, Z., Nemitz, E., Rogiers, N., Sanz, M.J., Siegwolf, R.T.W., Susiluoto, S., Sutton, M.,
39 1283 Tuba, Z., Ugolini, F., Valentini, R., Zorer, R., Cernusca, A., 2008. Biotic, abiotic, and
40 1284 management controls on the net ecosystem CO₂ exchange of European mountain
41 1285 grassland ecosystems. *Ecosystems* 11, 1338–1351. doi:10.1007/s10021-008-9196-2
42
43 1286 Wu, J., van der Linden, L., Lasslop, G., Carvalhais, N., Pilegaard, K., Beier, C., Ibrom, A., 2012.
44 1287 Effects of climate variability and functional changes on the interannual variation of the
45 1288 carbon balance in a temperate deciduous forest. *Biogeosciences* 9, 13–28.
46 1289 doi:10.5194/bg-9-13-2012
47
48 1290 Xiao, J., Chen, J., Davis, K.J., Reichstein, M., 2012. Advances in upscaling of eddy covariance
49 1291 measurements of carbon and water fluxes. *Journal of Geophysical Research* 117, G00J01.
50 1292 doi:10.1029/2011JG001889
51
52 1293 Xiao, J., Zhuang, Q., Liang, E., Shao, X., McGuire, A.D., Moody, A., Kicklighter, D.W., Melillo, J.M.,
53 1294 2009. Twentieth-century droughts and their impacts on terrestrial carbon cycling in
54 1295 China. *Earth Interactions* 13, 1–31. doi:10.1175/2009EI275.1
55
56 1296 Zeeman, M.J., Hiller, R., Gilgen, A.K., Michna, P., Plüss, P., Buchmann, N., Eugster, W., 2010.
57 1297 Management and climate impacts on net CO₂ fluxes and carbon budgets of three
58 1298 grasslands along an elevational gradient in Switzerland. *Agricultural and Forest*

1
2
3
4 1299 Meteorology 150, 519–530. doi:10.1016/j.agrformet.2010.01.011
5 1300
6
7
8
9
10
11
12
13
14
15
16
17
18
19
20
21
22
23
24
25
26
27
28
29
30
31
32
33
34
35
36
37
38
39
40
41
42
43
44
45
46
47
48
49
50
51
52
53
54
55
56
57
58
59
60
61
62
63
64
65

Tables

Table 1. Location, climate and management of the grassland study sites.

Country	Site	ID	Years	Geographical settings			Climate			Source
				Latitude	Longitude	Elevation(m a.s.l.)	Mean air temperature (°C)	Precipitation total (mm yr ⁻¹)		
France	Laqueuille	FRL.aq1	2004-2010	45° 38' N	02° 44' E	1040	7.8	1072	Klumpp et al. (2011)	
		FRL.aq2	2004-2010							
Germany	Grillenbourg	DEGri	2004-2008	50° 57' N	13° 30' E	375	8.5	946	Prescher et al. (2010)	
Hungary	Bugac-Pusztá	HUBug	2003-2008	46° 41' N	19° 36' E	140	10.2	520	Pintér et al. (2008)	
Ireland	Dripsey	IEDri	2003-2005	51° 59' N	08° 45' W	195	9.6	1271	Byrne and Kiely (2006)	
Italy	Amplero	ITAmp	2003-2007	41° 52' N	13° 38' E	884	9.4	781	Wohlfahrt et al. (2008)	
		ITMbo	2003-2007	46° 00' N	11° 02' E	1550	5.2	1003	Wohlfahrt et al. (2008)	
Portugal	Mitra	PTMi2	2005-2007	38° 32' N	08° 00' W	190	14.3	627	Aires et al. (2008)	
Spain	Vall d'Alinya	ESVDA	2004-2008	42° 12' N	01° 26' W	1770	6.2	908	Wohlfahrt et al. (2008)	
Switzerland	Oensingen	CHOe1	2002-2009	47° 17' N	07° 44' E	450	9.3	1197	Ammann et al. (2007)	
The Netherlands	Cabauw	NLCa1	2004-2007	51° 57' N	04° 54' W	0.7	10	800	Jacobs et al. (2007)	
United Kingdom	Easter Bush	UKEBu	2002-2008	55° 52' N	03° 02' W	190	9.0	956	Soussana et al. (2007a)	

Table 2. Soil properties and management of the grassland study sites (ID as in Table 1)

ID	Management (average)										Soil properties for the whole soil profile ¹				
	Utilization ² (yr ⁻¹)	Cuts (yr ⁻¹)	Nitrogen fertilization		Grazing			Clover fraction	Soil depth (m)	Soil texture					
			Events (yr ⁻¹)	Total amount (kg N ha ⁻¹ yr ⁻¹)	Stocking rate (LSU ³ ha ⁻¹ yr ⁻¹)	Duration (d yr ⁻¹)	Sand (%)			Silt (%)	Clay (%)	Bulk density (t m ⁻³)			
FRLaq1	Intensive	-	3	210	1.10	160	0.12	0.7	27	53	20	0.87			
FRLaq2	Extensive	-	-	-	0.60	160	-	-	-	-	-	-			
DEGri	Intensive	2-3	-	-	-	-	0.20	0.7	13	79	8	1.06			
BUG	Extensive	-	-	-	0.30	180	0.10	0.6	85	6	9	1.08			
IEDri	Intensive	-	3	280	0.72	150	0.17	0.7	52	27	21	1.19			
ITAmp	Intensive	-	-	-	0.50	200	0.20	0.7	12	33	55	0.92			
ITMbo	Extensive	1	-	-	-	-	0.20	0.7	44	39	17	1.04			
PTMi2	Extensive	-	-	-	1.46	70	0.00	0.7	55	35	10	1.12			
ESVDA	Extensive	-	-	-	0.18	120	0.10	0.6	15	50	35	0.87			
OEN	Intensive	3-4	4	214	-	-	0.25	1.0	24	33	43	1.15			
UKEBu	Extensive	-	4	200	0.65	160	0.00	0.7	12	24	62	1.47			
NLCa1	Intensive	-	3	225	0.60	180	0.00	0.7	45	25	30	1.19			

¹ Soil properties were obtained as the mean of six layers. Simulations make use of basic information for each layer.

² The classification into "extensive" or "intensive" grasslands was based on fertilizing intensity, the number of cuts, cattle density and/or grazing duration, which reflect the socio-economic environment in each country.

³ Livestock Standard Unit: standard measurement unit allowing the aggregation of various categories of livestock (species, sex and age) in order to enable them to be compared, related to the animals' feed requirements, using as a reference unit (=1 LSU) a dairy cow producing 3000 kg of milk annually, without additional concentrated feedstuffs (EC, 2008).

Table 3. Summary of the PaSim eco-physiological parameters considered in this study. For each parameter, three sets of values are reported: two from the calibration obtained in previous studies (P_temp, Oensingen and P_perm, Laqueuille, after Calanca et al., 2007 and Vuichard et al., 2007b) and one from the calibration performed in this study (P_redef). Greyed areas indicate the recalibrated parameters.

Name	Unit	Parameters			Values			Description
		P_temp (Oensingen)	P_perm (Laqueuille)	P_redef	P_temp (Oensingen)	P_perm (Laqueuille)	P_redef	
Fractional C content of root structural dry matter ($f_{C,rt}$)	kg C kg ⁻¹ DM	0.5	0.43	0.43	0.5	0.43	0.43	These parameters multiply the root and shoot growth rates, respectively, to obtain the C substrate variation.
Fractional C content of shoot structural dry matter ($f_{C,sh}$)	kg C kg ⁻¹ DM	0.39	0.435	0.435	0.39	0.435	0.435	
Parameter of the fractional N content of new plant structural dry matter ($f_{N,pl}$)	kg N kg ⁻¹ DM	0.022	0.018	0.018	0.022	0.018	0.018	This parameter is used to derive the nitrogen concentration of newly produced structural dry matter.
Maximum canopy height	m	0.35	0.707	0.707	0.35	0.707	0.707	It determines the canopy height to calculate the latent and sensible heat fluxes from the canopy and the soil surface.
Shoot turnover rate at 20 °C (%)	d ⁻¹	0.03	0.012	0.012	0.03	0.012	0.012	They represent the leaf and root life-spans at a constant temperature, used to calculate the flow of plant residue.
Root turnover rate at 20 °C (%)	d ⁻¹	0.05	0.048	0.048	0.05	0.048	0.048	
Fraction of fibres in ingested ears (NDF_{ear})	-	0.8	0.742	0.742	0.8	0.742	0.742	These parameters represent the proportion of fibre (NDF) in the ingested tissues (ear, lamina, sheath/stem).
Fraction of fibres in ingested blades (NDF_{lam})	-	0.6	0.542	0.542	0.6	0.542	0.542	
Fraction of fibres in ingested stems and sheaths (NDF_{stem})	-	0.7	0.642	0.642	0.7	0.642	0.642	
Maximum plant N concentration ($F_{N,max}$)	kg N kg ⁻¹ DM	0.045	0.03	0.03	0.045	0.03	0.03	This parameter limits N absorption by plant.

Digestible neutral detergent fibres of ears - age 1 (DNDF _{ears1})	kg digestible fibres kg ⁻¹ fibres	0.76	0.93	0.93	They represent the influence of developmental stage (the end of ear emergence marking the transition from the reproductive to the vegetative stage) on the light-saturated leaf photosynthetic rate (defined at standard conditions of temperature, atmospheric CO ₂ concentration and plant nitrogen concentration), which is a component of the rate of canopy photosynthesis.
Digestible neutral detergent fibres of ears - age 2 (DNDF _{ears2})	kg digestible fibres kg ⁻¹ fibres	0.48	0.68	0.68	
Digestible neutral detergent fibres of ears - age 3 (DNDF _{ears3})	kg digestible fibres kg ⁻¹ fibres	0.3	0.44	0.44	
Digestible neutral detergent fibres of ears - age 4 (DNDF _{ears4})	kg digestible fibres kg ⁻¹ fibres	0.26	0.38	0.38	
Light-saturated leaf photosynthetic rate for reproductive stage (<i>pmco2rep</i>)	μmol C m ⁻² s ⁻¹	22.6666	16.723	19.723	
Light-saturated leaf photosynthetic rate for vegetative stage (<i>pmco2veg</i>)	μmol C m ⁻² s ⁻¹	15	11.099	13.099	
Maximum specific leaf area (<i>slam</i>)	m ² kg ⁻¹	33.5	25	29	This is the maximum value of specific leaf area, defined as the ratio of leaf area to dry weight, used to derive canopy leaf area from leaf biomass.
Temperature dependence factor of the soil respiration (<i>m_{rr}</i>)	-	2	2	0.7	It multiplies the temperature-dependent function ¹ to estimate soil respiration.

$$f(T_a) = \frac{(T_a - T_0)^{q_{FT}} \cdot (T'_0 - T_a)}{(T_{ref} - T_0)^{q_{FT}} \cdot (T'_0 - T_{ref})}, T_0 \leq T_a \leq T'_0$$

0 otherwise

where T_a (°C) is air temperature; T_0 (°C), T'_0 (°C), T_{ref} (°C) are, respectively, the base air temperature, the ceiling air temperature at which

1
2
3
4
5
6
7
8
9
10
11
12
13
14
15
16
17
18
19
20
21
22
23
24
25
26
27
28
29
30
31
32
33
34
35
36
37
38
39
40
41
42
43
44
45
46
47
48
49
50
51
52
53
54
55
56
57
58
59
60
61
62
63
64
65

processes cease, and reference air temperature at which the maximum rate of respiration occurs; q_{rr} (unitless) is a shape parameter. Reference values for soil respiration are: $T_0=0$ °C, $T_0=45$ °C, $T_{ref}=20$ °C, $q_{rr}=2$.

Table 4. Model performance measurement indices.

Performance measure	Equation	Unit	Value range and purpose	Reliability	
				criterion	source
Coefficient of determination (R^2) of the linear regression estimates versus measurements (Addiscott and Whitmore, 1987)	$R^2 = \frac{\sum_{i=1}^n (P_i - O_i) \cdot (O_i - \bar{O})}{\sqrt{\sum_{i=1}^n (P_i - \bar{P})^2 \cdot \sum_{i=1}^n (O_i - \bar{O})^2}}$	-	0 (absence of fit of the regression line) to 1 (perfect fit of the regression line): the closer the values are to 1, the better the model	>0.8	De Jager (1994)
IA, index of agreement (Willmott and Wicks, 1980)	$IA = 1 - \frac{\sum_{i=1}^n (P_i - O_i)^2}{\sum_{i=1}^n (P_i - \bar{O} + O_i - \bar{O})^2}$	-	0 (absence of agreement) to 1 (perfect agreement): the closer the values are to 1, the better the model	>0.8	De Jager (1994)
RMSE, root mean square error (Fox, 1981)	$RMSE = \sqrt{\frac{\sum_{i=1}^n (P_i - O_i)^2}{n}}$	unit of the variable	0 (optimum) to positive infinity: the smaller RMSE, the better the model performance	-	-
MB, mean bias (Addiscott and Whitmore, 1987)	$MB = \frac{\sum_{i=1}^n (P_i - O_i)}{n}$	unit of the variable	negative infinity (underestimation) to positive infinity (overestimation): the closer the values are to 0, the better the model	-	-
ME, modelling efficiency (Nash and Sutcliffe, 1970)	$ME = 1 - \frac{\sum_{i=1}^n (P_i - O_i)^2}{\sum_{i=1}^n (O_i - \bar{O})^2}$	-	negative infinity to 1 (optimum): the closer the values are to 1, the better the model	>0.5	Moriassi et al. (2007)

Table 5. Model performances across grassland sites (ID as in Table 1) based on different evaluation indices (as in Table 4) calculated on weekly aggregated data.

Site ID	GPP						RECO						ET							
	NEE		RMSE		IA	R ²	BIAS		RMSE		IA	ME	R ²	BIAS		RMSE		IA	ME	R ²
	BIAS	RMSE	g C week ⁻¹ m ⁻²	g C week ⁻¹ m ⁻²	g C week ⁻¹ m ⁻²	g C week ⁻¹ m ⁻²	g C week ⁻¹ m ⁻²	g C week ⁻¹ m ⁻²	g C week ⁻¹ m ⁻²	g C week ⁻¹ m ⁻²	g C week ⁻¹ m ⁻²	g C week ⁻¹ m ⁻²	g C week ⁻¹ m ⁻²	g C week ⁻¹ m ⁻²	mm week ⁻¹	mm week ⁻¹	mm week ⁻¹	mm week ⁻¹	mm week ⁻¹	mm week ⁻¹
CHOe1	-6.07	15.83	0.91	0.69	0.73	-10.35	12.90	0.88	0.58	0.88	0.58	0.88	0.88	-1.69	3.14	0.96	0.84	0.891		
ITMbo	-2.22	10.89	0.96	0.85	0.86	0.89	12.22	0.93	0.59	0.86	0.59	0.86	0.93	-1.26	2.67	0.97	0.89	0.926		
DEGri	-0.10	9.13	0.95	0.81	0.83	-1.53	11.74	0.88	0.44	0.63	0.44	0.63	0.88	1.23	3.45	0.92	0.60	0.827		
UKEBu	-1.85	10.53	0.95	0.79	0.81	-2.88	10.44	0.91	0.68	0.72	0.68	0.72	0.91	0.66	3.95	0.82	0.37	0.465		
IEDri	5.03	13.40	0.93	0.66	0.83	2.27	12.58	0.91	0.61	0.70	0.61	0.70	0.91	-1.84	2.65	0.94	0.76	0.887		
HUBug	9.24	16.79	0.83	-0.02	0.64	7.95	15.12	0.80	-0.59	0.70	-0.59	0.70	0.80	1.74	6.03	0.86	0.24	0.645		
ITAmp	-9.06	16.18	0.74	0.10	0.40	-9.03	14.44	0.61	-0.07	0.39	-0.07	0.39	0.61	-2.31	5.08	0.88	0.57	0.676		
ESVDA	0.94	6.59	0.92	0.58	0.77	1.43	5.04	0.91	0.52	0.82	0.52	0.82	0.91	0.78	2.82	0.95	0.73	0.864		
FRLq1	-2.94	10.07	0.96	0.85	0.87	-2.87	11.42	0.93	0.65	0.80	0.65	0.80	0.93	-4.12	5.93	0.86	0.47	0.728		
FRLq2	5.35	14.84	0.93	0.59	0.85	4.51	13.66	0.90	0.35	0.84	0.35	0.84	0.90	-1.49	3.97	0.94	0.75	0.799		
PTMi2	-3.89	11.21	0.82	0.47	0.53	-2.14	8.39	0.78	0.43	0.46	0.43	0.46	0.78	3.79	8.21	0.61	-2.04	0.316		
NLCa1	4.27	14.04	0.92	0.57	0.80	6.55	16.23	0.88	0.27	0.76	0.27	0.76	0.88	-1.18	2.87	0.96	0.82	0.888		
Site ID	NEE						SWC						SoiIT							
	RMSE		IA	ME	R ²	BIAS		RMSE		IA	ME	R ²	BIAS		RMSE		IA	ME	R ²	
	BIAS	RMSE	g C week ⁻¹ m ⁻²	g C week ⁻¹ m ⁻²	g C week ⁻¹ m ⁻²	g C week ⁻¹ m ⁻²	g C week ⁻¹ m ⁻²	g C week ⁻¹ m ⁻²	g C week ⁻¹ m ⁻²	g C week ⁻¹ m ⁻²	g C week ⁻¹ m ⁻²	g C week ⁻¹ m ⁻²	g C week ⁻¹ m ⁻²	g C week ⁻¹ m ⁻²	g C week ⁻¹ m ⁻²	g C week ⁻¹ m ⁻²	g C week ⁻¹ m ⁻²	g C week ⁻¹ m ⁻²	g C week ⁻¹ m ⁻²	
CHOe1	-4.10	12.27	0.80	0.25	0.43	5.04	7.78	0.69	0.21	0.72	0.21	0.72	0.69	-3.19	4.06	0.91	0.71	0.91		
ITMbo	3.11	17.13	0.48	-0.92	0.02	-15.84	16.89	0.41	-5.20	0.26	-5.20	0.26	0.41	-0.80	3.88	0.94	0.64	0.89		
DEGri	-1.43	7.72	0.83	0.44	0.50	-4.24	6.23	0.83	0.50	0.80	0.50	0.80	0.83	-3.63	4.35	0.92	0.55	0.94		
UKEBu	-1.03	8.90	0.74	0.21	0.31	1.69	5.36	0.75	0.48	0.68	0.48	0.68	0.75	-3.06	4.00	0.87	0.34	0.82		
IEDri	-2.76	8.03	0.81	0.25	0.47	-1.60	2.64	0.82	0.49	0.72	0.49	0.72	0.82	-1.24	1.73	0.94	0.71	0.93		
HUBug	-1.29	6.27	0.84	0.45	0.52	7.10	8.44	0.55	-1.34	0.34	-1.34	0.34	0.55	-0.93	2.06	0.98	0.92	0.96		
ITAmp	0.19	9.81	0.72	0.14	0.27	3.52	7.55	0.70	0.21	0.38	0.21	0.38	0.70	-0.94	5.96	0.90	0.39	0.77		
ESVDA	0.49	6.04	0.65	-0.81	0.19	4.47	6.05	0.68	-0.14	0.48	-0.14	0.48	0.68	1.95	2.46	0.97	0.88	0.96		

FRLq1	0.08	9.88	0.76	0.32	0.35	4.45	6.06	0.60	-0.57	0.29	-1.36	2.42	0.96	0.85	0.911
FRLq2	-0.83	9.34	0.76	0.34	0.37	5.03	7.69	0.60	-0.24	0.29	-1.75	2.53	0.95	0.79	0.905
PTMi2	1.75	7.90	0.68	-0.51	0.25	0.28	8.83	0.61	0.39	0.78	-1.45	2.86	0.97	0.91	0.944
NLCa1	2.29	10.68	0.68	-0.79	0.28	-16.50	19.98	0.49	-1.67	0.29	NA	NA	NA	NA	NA

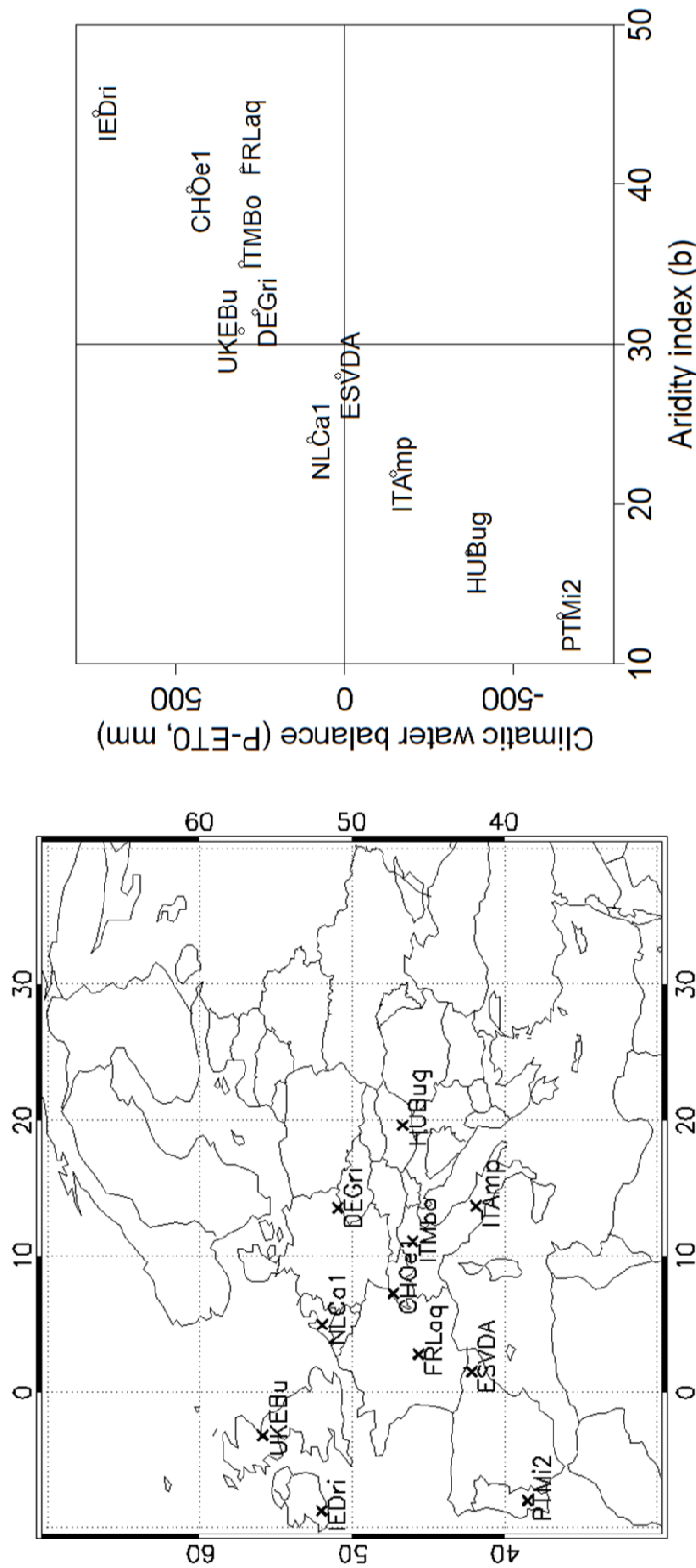


Fig 1. Geographic location (left) and classification (right) of grassland sites (ID as in Table 1) with respect to two indices (climatic water balance and De Martonne-Gottmann aridity index) of water availability. For the aridity index b , (De Martonne, E, 1942), the following range limits discriminate between thermo-pluviometric conditions associated with aridity gradients: $b < 5$: extreme aridity; $5 \leq b \leq 14$: aridity; $15 \leq b \leq 19$: semi-aridity; $20 \leq b \leq 29$: sub-humidity; $30 \leq b \leq 59$: humidity; $b > 59$: strong humidity (Diodato and Ceccarelli, 2004).

Figures:

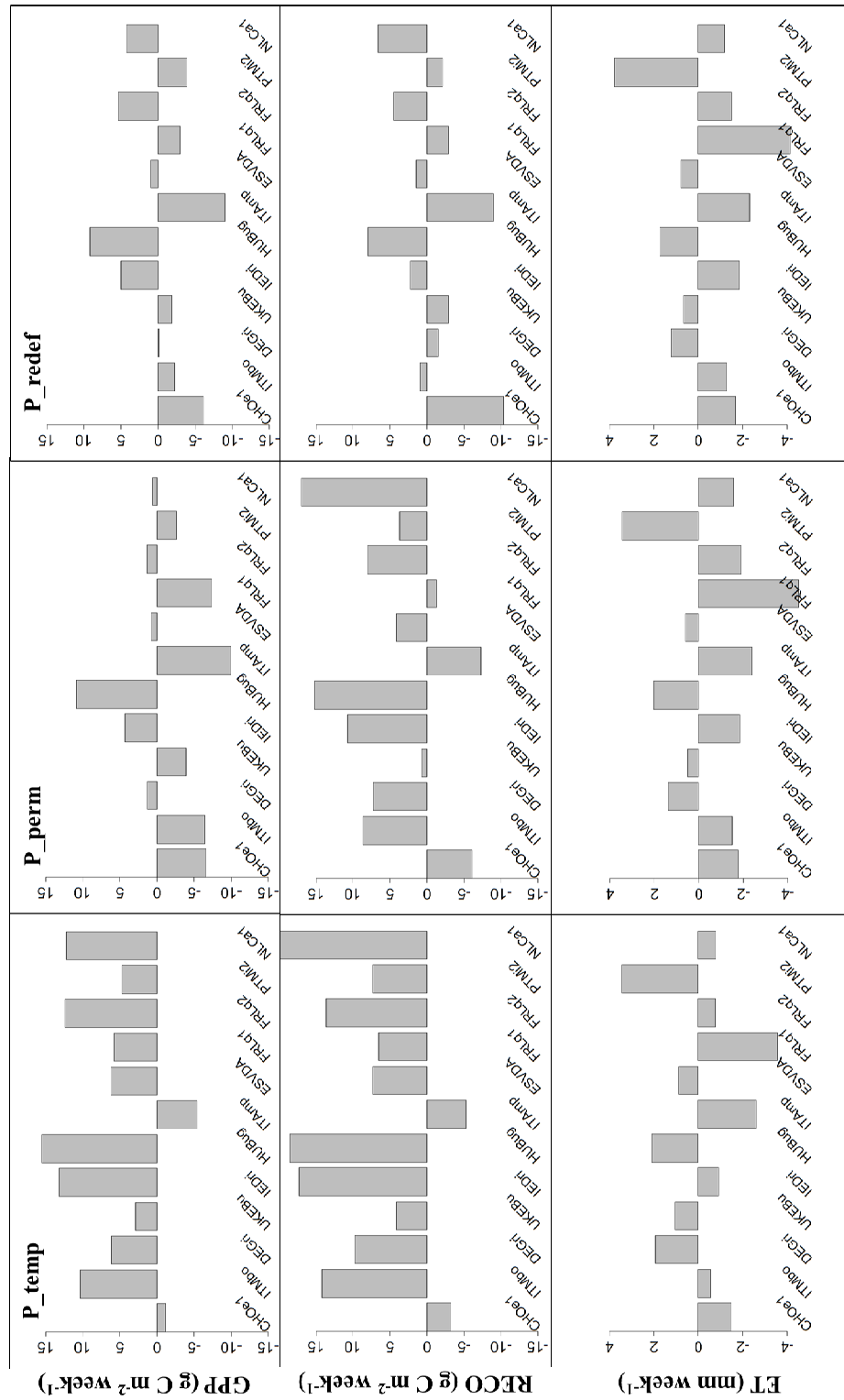
1
2
3
4
5
6
7
8
9
10
11
12
13
14
15
16
17
18
19
20
21
22
23
24
25
26
27
28
29
30
31
32
33
34
35
36
37
38
39
40
41
42
43
44
45
46
47
48
49
50
51
52
53
54
55
56
57
58
59
60
61
62
63
64
65

Fig 2. The mean bias of weekly values of GPP, RECO ($\text{g C m}^{-2} \text{ week}^{-1}$) and ET (mm week^{-1}), using three sets of parameter values: for temporary grasslands as established at Oensingen, Switzerland (P_temp, left), for permanent grasslands as established at Laqueuille, France (P_perm, middle), and the common set established in this study (P_redef, right).

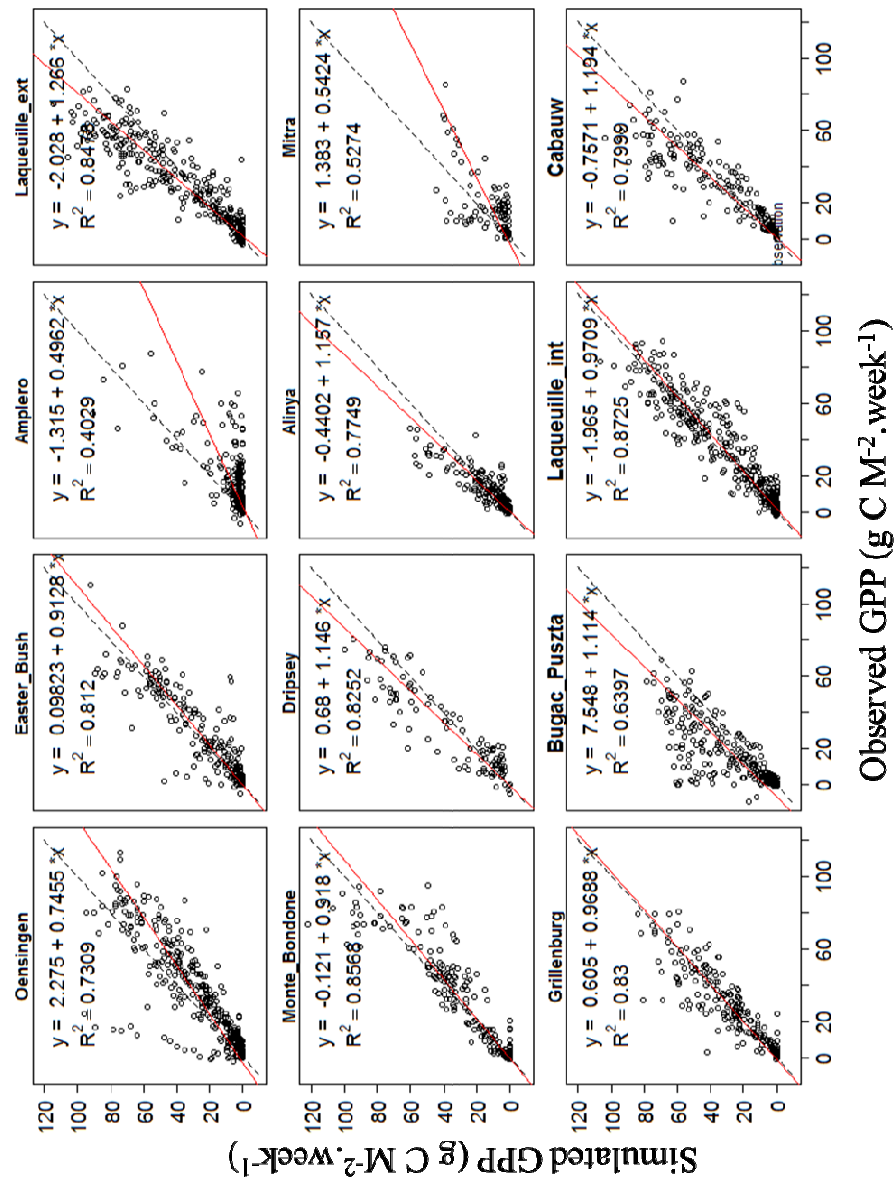


Fig. 3. Scatter plots of simulated versus measured GPP weekly values. The dashed line is the 1:1 line. The solid red line represents the regression equation. The goodness-of-fit R^2 is the coefficient of determination of the regression equation.

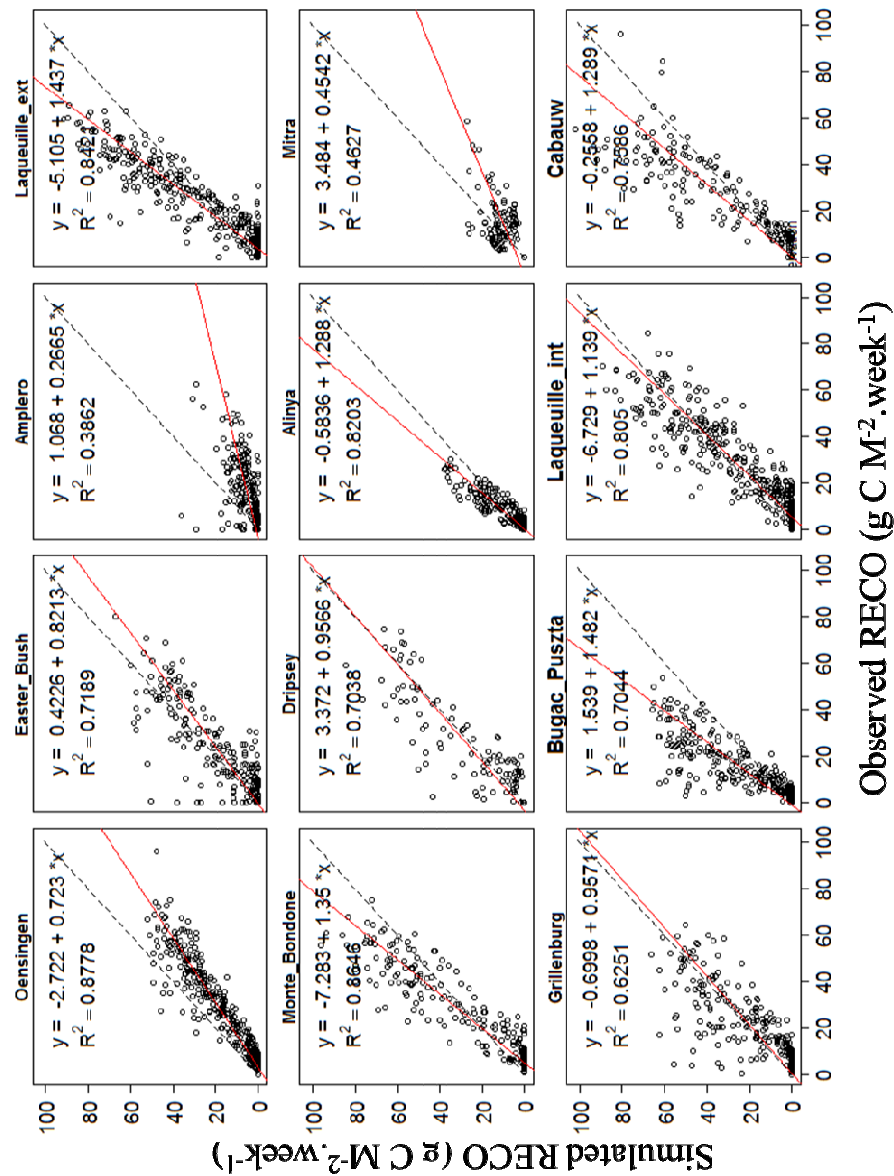


Fig. 4. Scatter plots of simulated versus measured RECO weekly values. The dashed line is the 1:1 line. The solid red line represents the regression equation. The goodness-of-fit R^2 is the coefficient of determination of the regression equation.

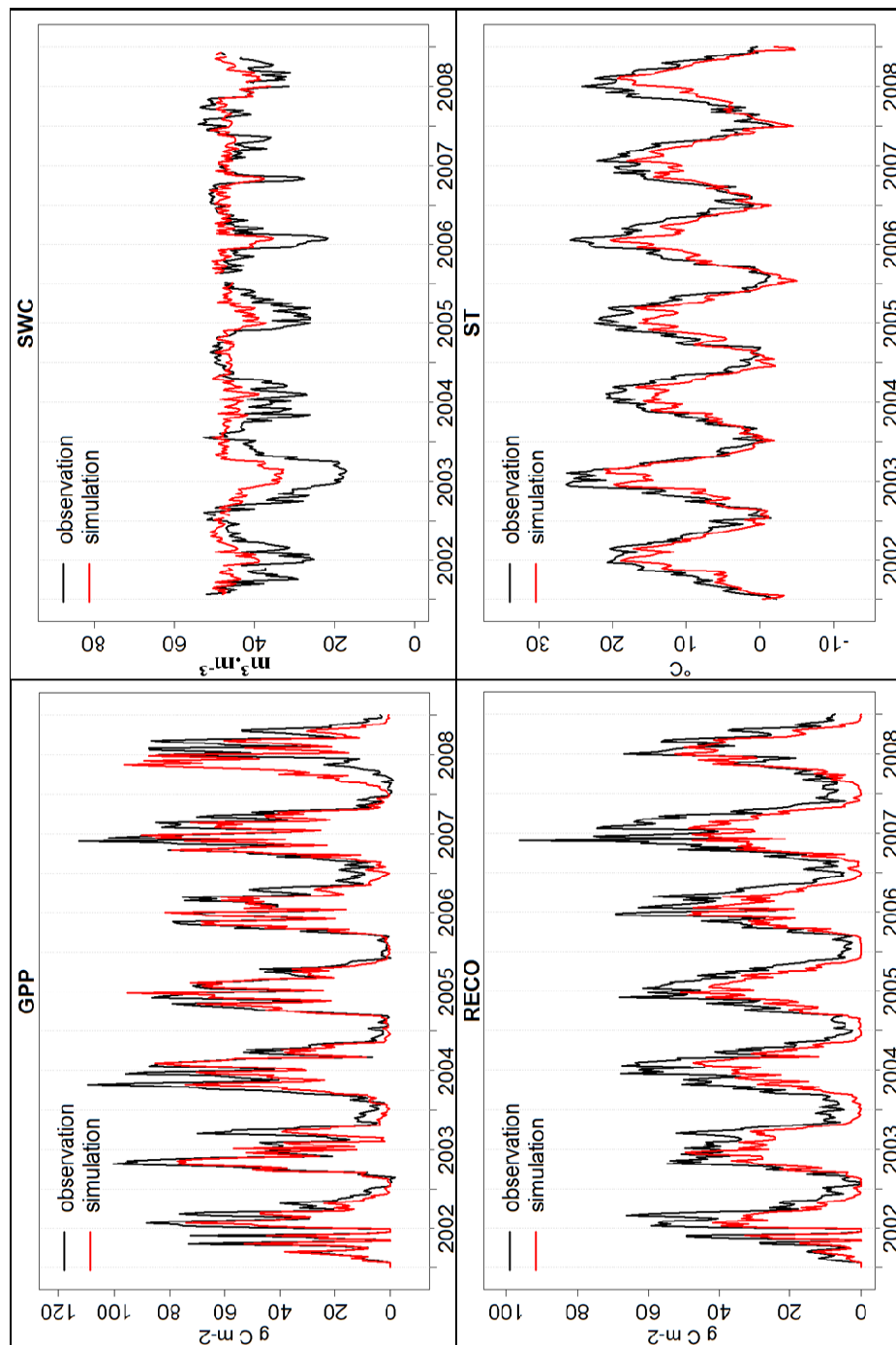
1
2
3
4
5
6
7
8
9
10
11
12
13
14
15
16
17
18
19
20
21
22
23
24
25
26
27
28
29
30
31
32
33
34
35
36
37
38
39
40
41
42
43
44
45
46
47
48
49
50
51
52
53
54
55
56
57
58
59
60
61
62
63
64
65

Fig. 5. The variability of simulated GPP, RECO, soil temperature (ST) and soil water content (SWC) against the observed data for Oensingen (Switzerland) weekly values.

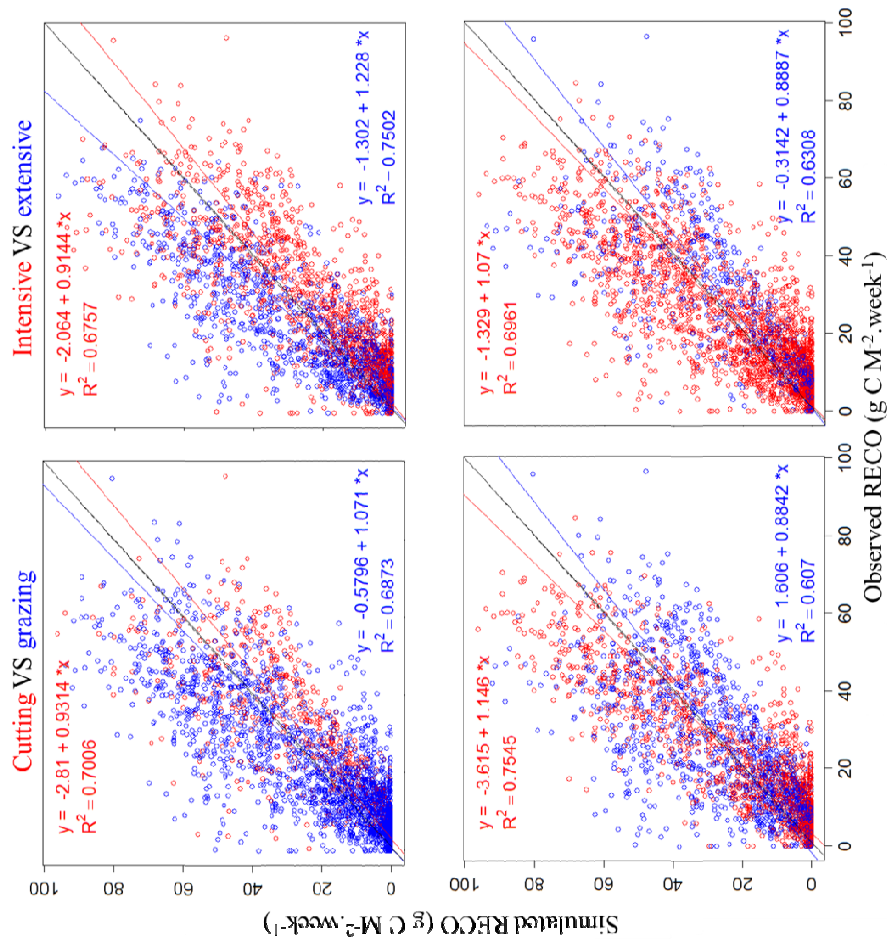


Fig. 6. Scatter plots of simulated with the redefined parameters versus measured RECO values (g C M⁻².week⁻¹) according to site characteristics and management practices. The goodness-of-fit R² is the coefficient of determination of the regression equation.

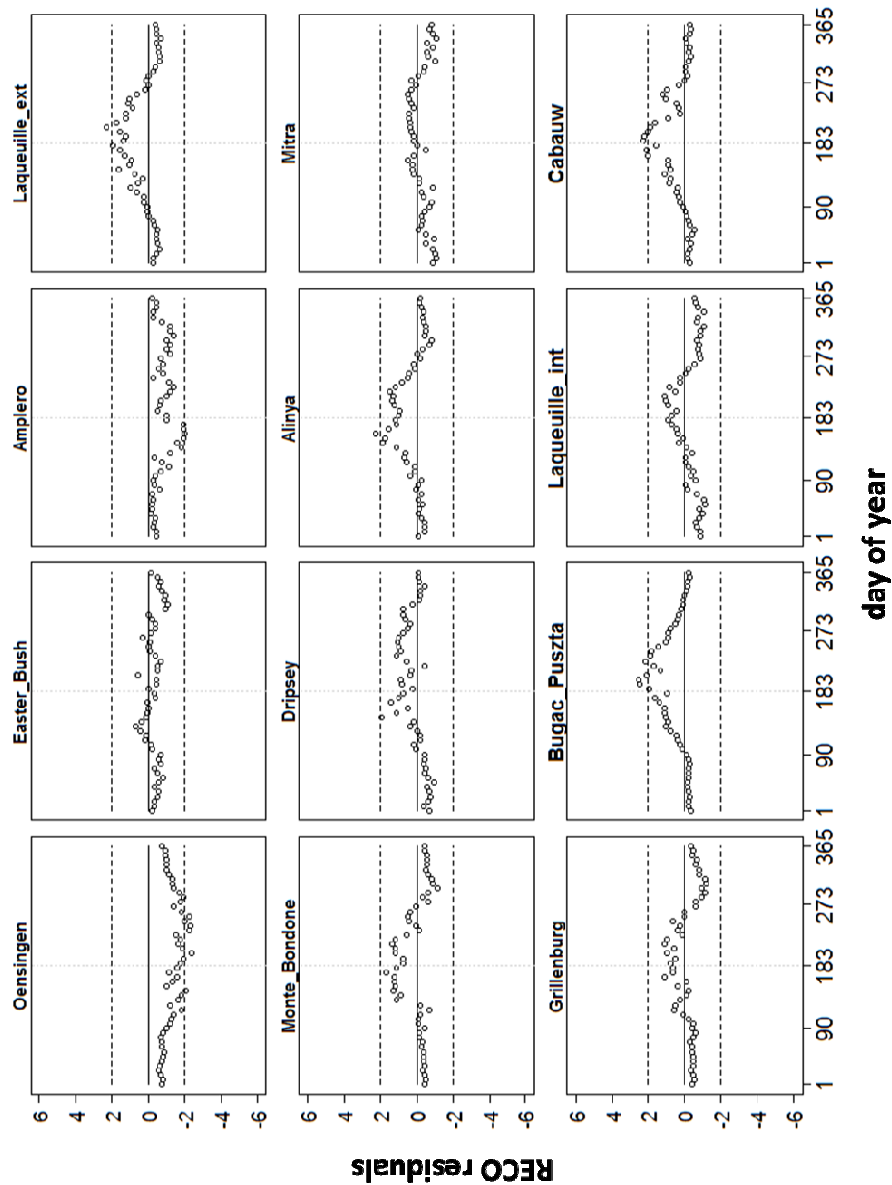


Fig. 7. Normalized residuals of RECO plotted versus day of year for each grassland site. Each point is the average of residuals for all years divided by the standard deviation. Horizontal lines represent the 95% confidence limits.

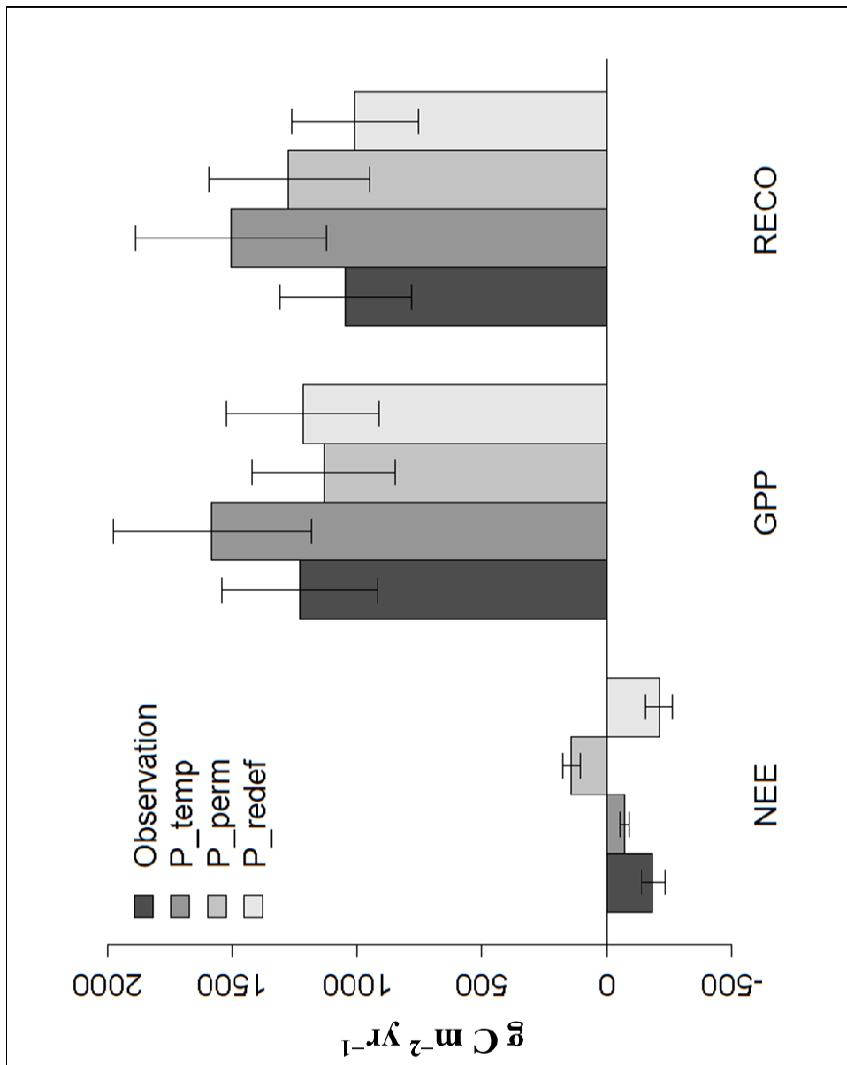


Fig. 8. Comparison of observed and simulated carbon fluxes (NEE, GPP, RECO; $\text{g C m}^{-2} \text{yr}^{-1}$) with different parameter values (default for Oensingen (P_temp) and Laqueuille (P_perm), and new parameter values (P_redef)). The values are averaged across all grassland sites.

1
2
3
4
5
6
7
8
9
10
11
12
13
14
15
16
17
18
19
20
21
22
23
24
25
26
27
28
29
30
31
32
33
34
35
36
37
38
39
40
41
42
43
44
45
46
47
48
49
50
51
52
53
54
55
56
57
58
59
60
61
62
63
64
65

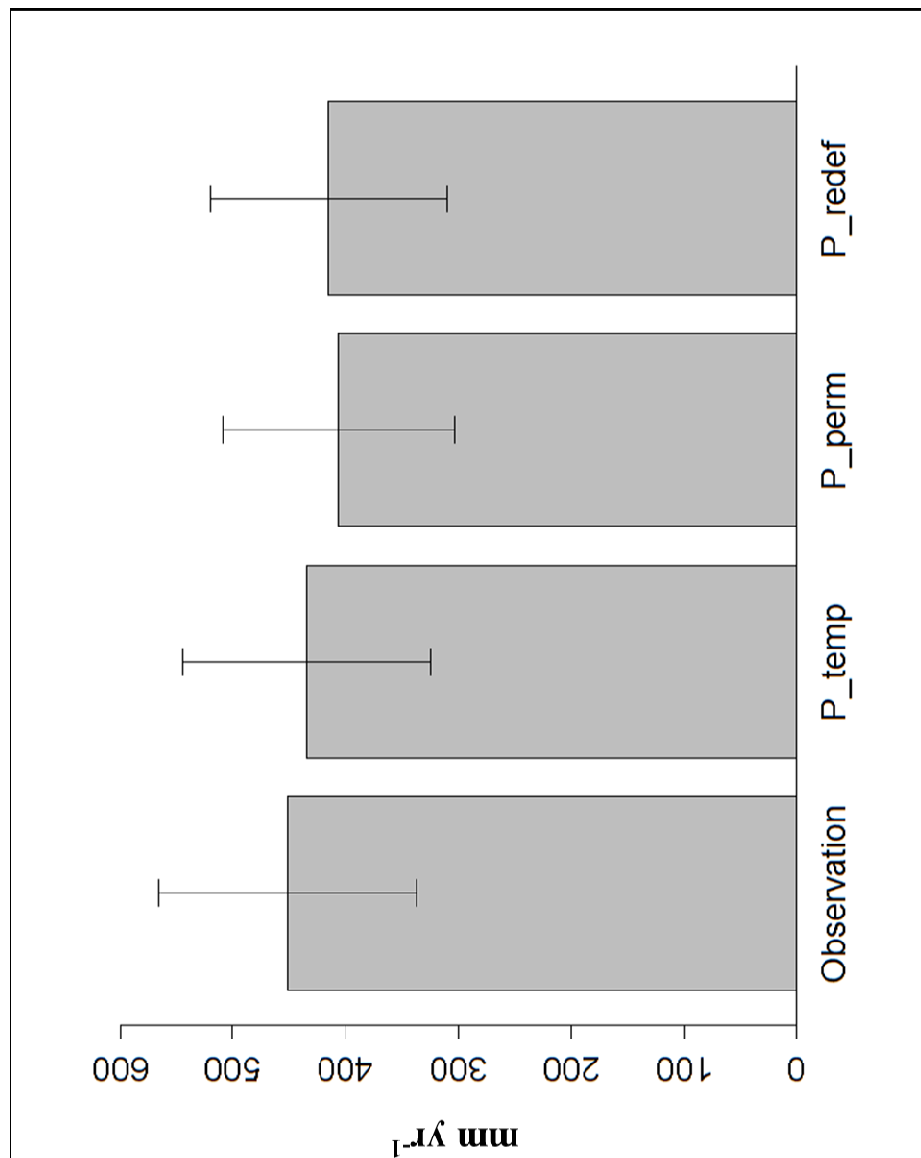


Fig. 9. Comparison of observed and simulated water fluxes (mm yr^{-1}) with different parameter values (default for Oensingen (P_temp) and Laqueuille (P_perm), and new parameter values (P_redef)). The values are averaged across all grassland sites.

1
2
3
4
5
6
7
8
9
10
11
12
13
14
15
16
17
18
19
20
21
22
23
24
25
26
27
28
29
30
31
32
33
34
35
36
37
38
39
40
41
42
43
44
45
46
47
48
49
50
51
52
53
54
55
56
57
58
59
60
61
62
63
64
65

Appendix G: support figures

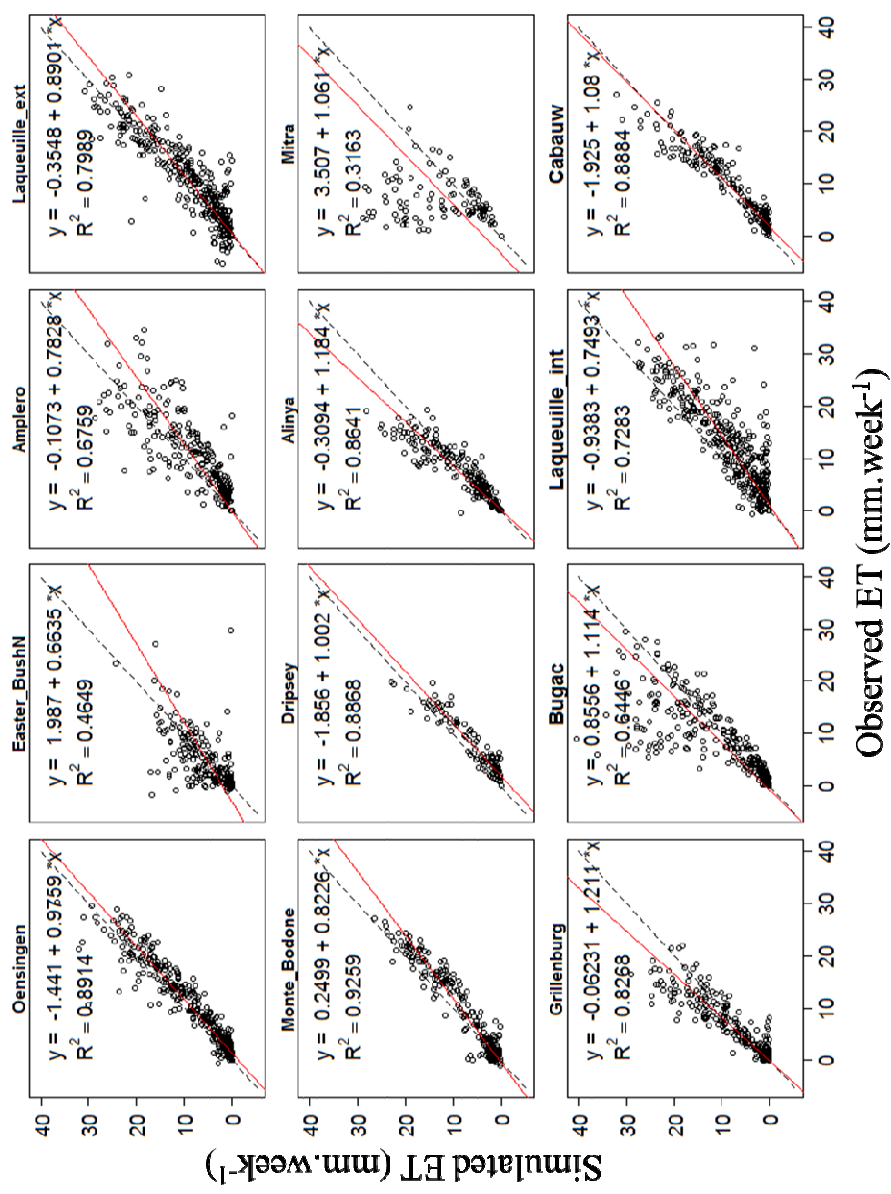


Fig. A1. Scatter plots of simulated versus measured ET weekly values.

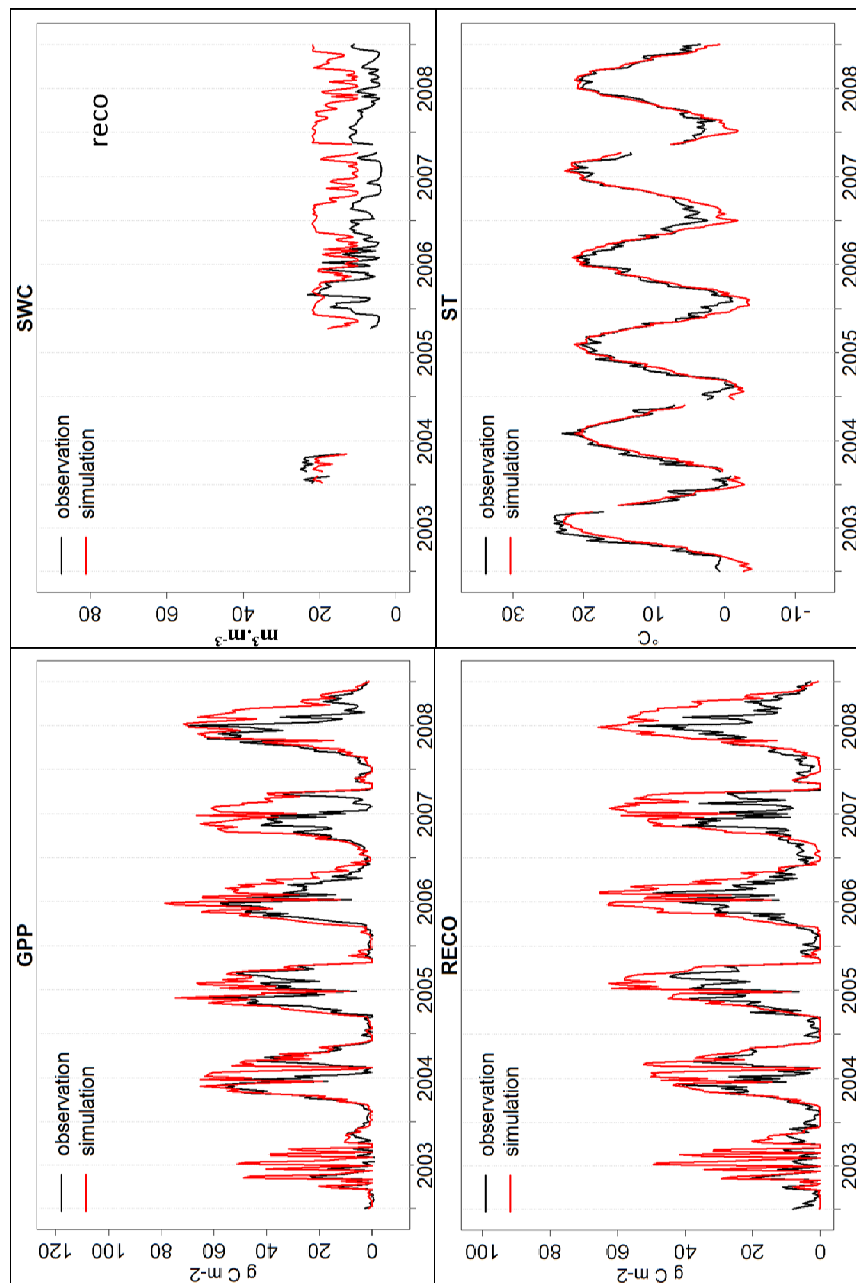


Fig. A2. The variability of simulated GPP, RECO, soil temperature (ST) and soil water content (SWC) against the observed data for Bugac-Pusztá (Hungary) weekly values.

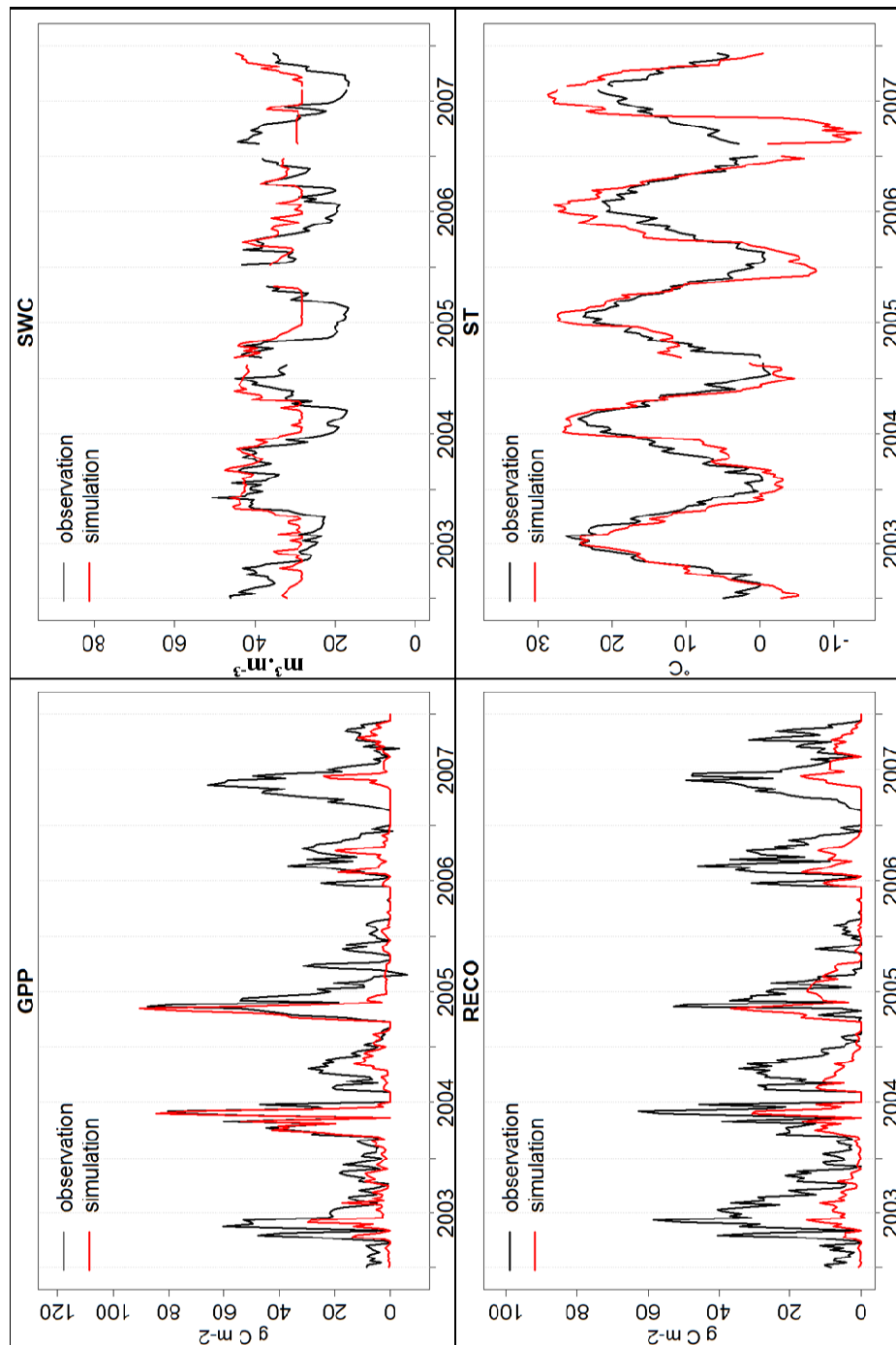
1
2
3
4
5
6
7
8
9
10
11
12
13
14
15
16
17
18
19
20
21
22
23
24
25
26
27
28
29
30
31
32
33
34
35
36
37
38
39
40
41
42
43
44
45
46
47
48
49
50
51
52
53
54
55
56
57
58
59
60
61
62
63
64
65

Fig. A3. The variability of simulated GPP, RECO, soil temperature (ST) and soil water content (SWC) against the observed data for Amplero (Italy) weekly values.

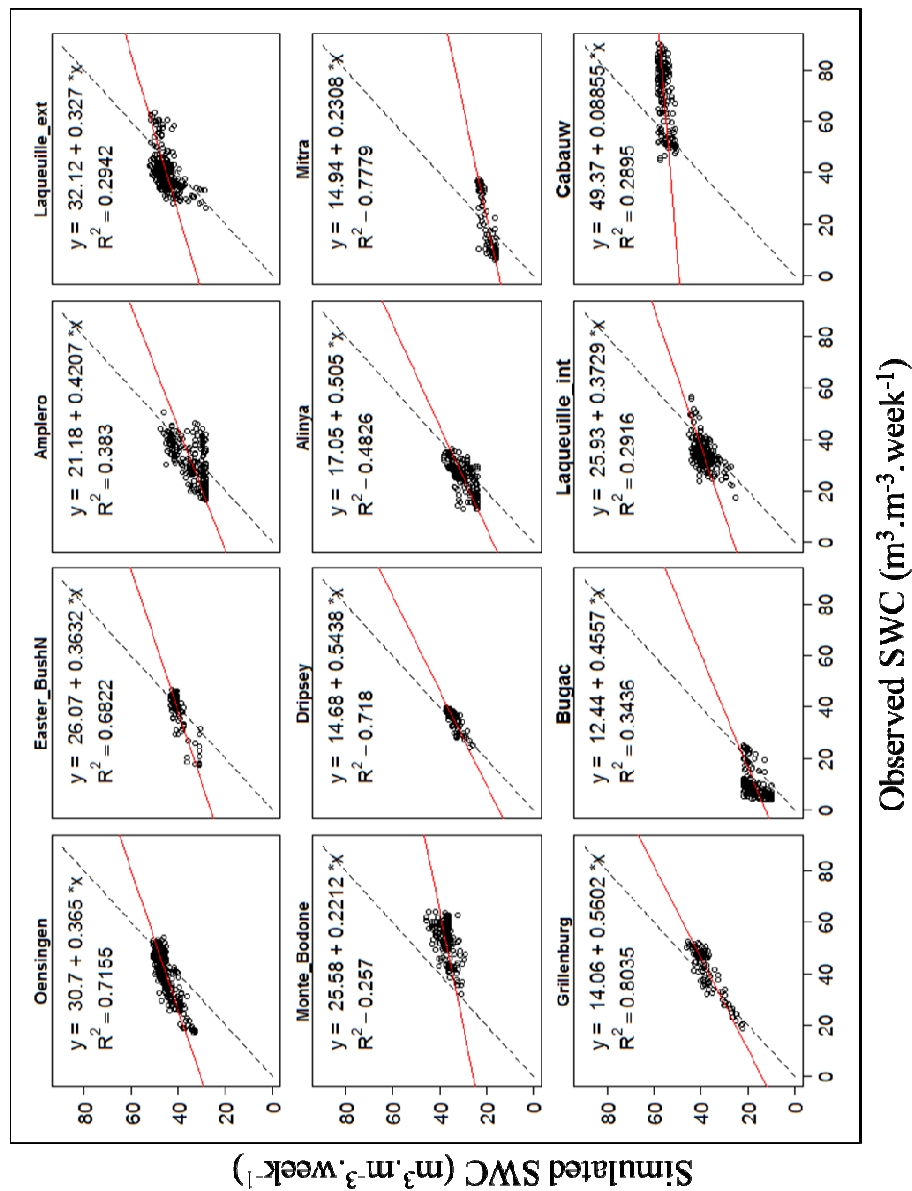
1
2
3
4
5
6
7
8
9
10
11
12
13
14
15
16
17
18
19
20
21
22
23
24
25
26
27
28
29
30
31
32
33
34
35
36
37
38
39
40
41
42
43
44
45
46
47
48
49
50
51
52
53
54
55
56
57
58
59
60
61
62
63
64
65

Fig. A4. Scatter plots of simulated versus measured soil water content in the top 10 centimetres.

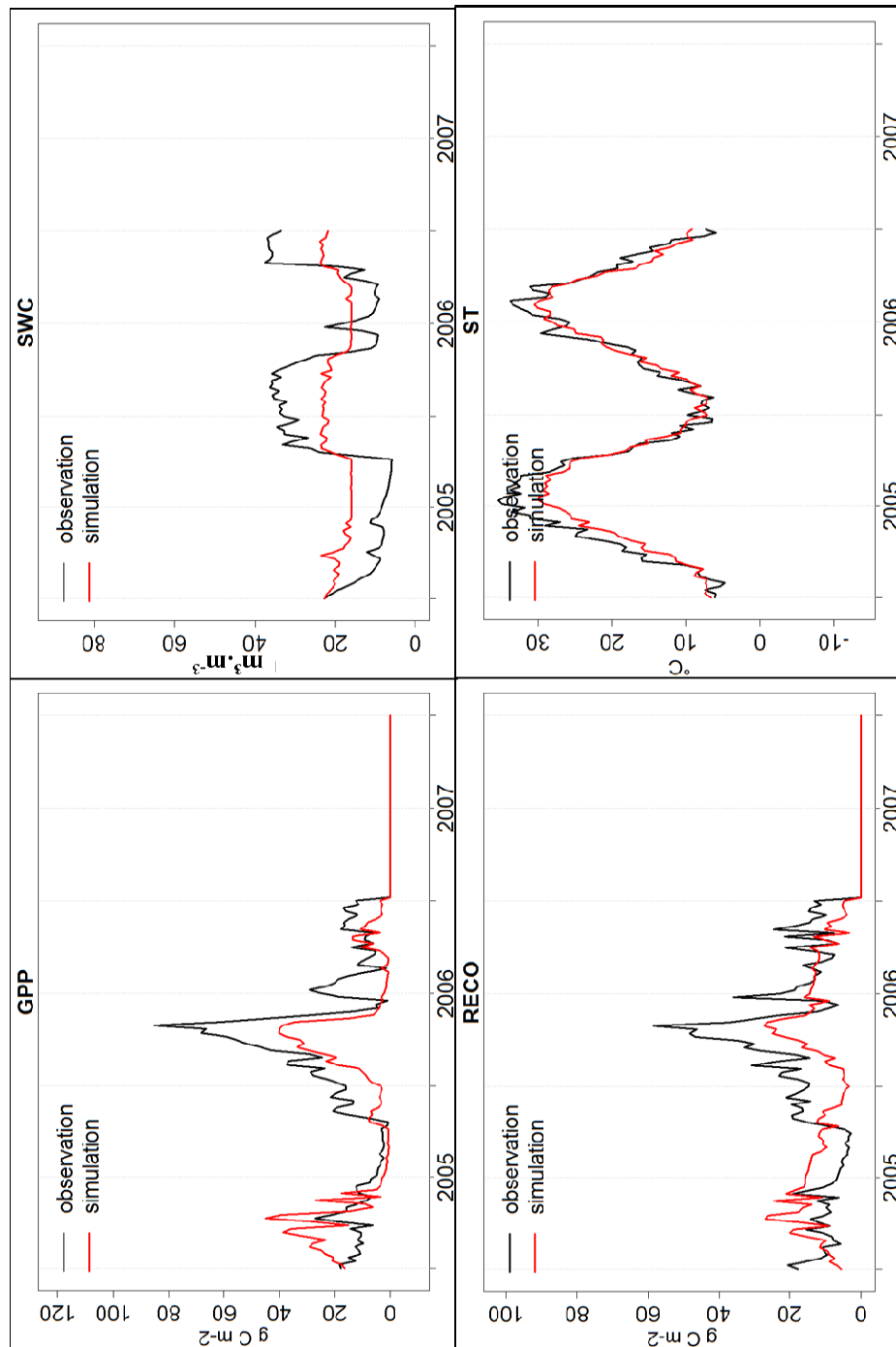
1
2
3
4
5
6
7
8
9
10
11
12
13
14
15
16
17
18
19
20
21
22
23
24
25
26
27
28
29
30
31
32
33
34
35
36
37
38
39
40
41
42
43
44
45
46
47
48
49
50
51
52
53
54
55
56
57
58
59
60
61
62
63
64
65

Fig. A5. The variability of simulated GPP, RECO, soil temperature (ST) and soil water content (SWC) against the observed data for Mitra (Portugal) weekly values.

Comment citer ce document :

Ma, S., Lardy, R., Graux, A.-I., Ben Touhami, H., Klumpp, K., Martin, R., Bellocchi, G. (2015). Regional-scale analysis of carbon and water cycles on managed grassland systems. *Environmental Modelling and Software*, 72, 356-371. DOI : 10.1016/j.envsoft.2015.03.007